Synthesis and Characterization of Purely Sulphonated Polysiloxane and Composite Membranes for High Temperature Fuel Cells

By

Nicole E. De Almeida

A thesis submitted to the school of graduate studies in partial fulfillment for the degree of Masters of Science

In

The Faculty of Science

Material Science

University of Ontario Institute of Technology
Oshawa, Ontario, Canada
April 2010

Abstract

Fuel cell technologies have developed high interest due to their ability to provide energy in an environmentally friendly method. Proton exchange membrane fuel cells (PEM-FCs) require a PEM for use, where the most accepted PEM used today is Nafion. Nafion is ideal due to its chemical durability and high proton conductivity however it is highly expensive and limited to 80˚C during operation. To target these issues two methods have been developed. One was to synthesize a new membrane material to replace Nafion based upon sulphonated polysiloxanes and the other was to improve Nafion by synthesizing a composite. Both of these methods involved the sulphonated silane 2-4-chlorosulphonylphenethyltrimethoxysilane. Methods to characterize membranes to observe their properties compared to Nafion were thermogravimetric analysis (TGA), Fourier transmission infrared spectroscopy (FT-IR), electrochemical impedance spectroscopy (used to determine proton conductivity) and fuel cell performance.

Acknowledgements

Firstly, I would like to thank my supervisor Dr. Brad Easton for all his help and guidance in this project. I send my thanks also to the Easton lab for all the aid they have given me as well as the numerous entertaining conversations.

My gratitude goes out to the funding I've received to help my research to NSERC, Ontario Research Fund, UOIT, OPIC, and the Canada Foundation for Innovation.

I'm very grateful to my family who have supported me in my endeavours thus far as if it was not for them I would have never made it this far. To my parents and grandmothers I'm eternally thankful for all your love and support thus far and hope to continue making you proud. To my sisters a special thanks for both of you for always being there.

My deepest thanks are to the Orangevillian crew whose enthusiasm and belief in me that I could accomplish this could never be thanked enough. They have all been a huge part in my successes to date.

A special acknowledgement is to my boyfriend Allen Pauric for his patience and helpfulness for the duration of this thesis. Your encouragement was the perfect motivation to pull me through and I cannot find the words to thank you enough.

Table of Contents

List of Tables

List of Figures

List of Abbreviations

CSPETMOS: 2-4-Chlorosulphonylphenethyltrimethoxysilane

DMDMOS: Dimethyldimethoxysilane

DS: Degree of Sulphonation

EIS: Electrochemical Impedance Spectroscopy

FT-IR: Fourier Transmission Infrared Spectroscopy

MEA: Membrane Electrode Assembly

PEM: Proton Exchange Membrane

PEM-FC: Proton Exchange Membrane Fuel Cell

PETMOS: Phenethyltrimethoxysilane

RH: Relative Humidity

SPPES: Sulphonatedphenethylsilane

SS: Sulphonated Silica

TGA: Thermogravimetric Analysis

Chapter One

Introduction

1.1: Fuel Cells

Alternative energy systems are needed in order to reduce green-house gasses in a form of sustainable energy. High temperature fuel cells, such as solid oxide fuel cells are used in power plants [1]. Low temperature fuel cells like direct methanol fuel cells and proton exchange membrane fuel cells are targeted for portable devices and automobiles respectively [2].

Proton exchange membrane fuel cells (PEMFCs) are devices that convert chemical energy into electrical energy by the use of a proton conducting polymer [3]. These types of fuel cells normally operate at low temperatures (80°C), which makes them suitable for portable applications (4, 5). Depicted in Figure 1.1 is a cross section of PEMFC that consist of an anode and cathode separated by solid proton exchange membrane (PEM). PEMFCs operate by having hydrogen introduced to the anode, which undergoes an oxidation to protons and electrons as seen in Equation 1.1 [4].

$$H_2 \rightarrow 2H^+ + 2e^- \quad E_o=0V \qquad \textbf{Equation 1. 1}$$

The protons travel through the PEM, while the electrons travel through an external circuit, generating electricity [4]. Electrons, protons, and oxygen recombine at the cathode to produce water as a product seen in Equation 1.2 [4, 6-7].

$$O_2 + 4H^+ + 4e^- \rightarrow 2H_2O \quad E_0=1.229 \qquad \textbf{Equation 1. 2}$$

1.1.1: Electrodes

The electrode of a PEMFC consists of platinum nanoparticles on a carbon support [8]. These electrode layers are used for more than just catalyzing the reactions. Electrode

layers are required to do three tasks, catalyze hydrogen oxidation and oxygen reduction reactions, allow reactant diffusion within electrodes, and to be electrically conductive [4]. Gas diffusion is required for the efficient transport of hydrogen and oxygen to the catalyst. Electrical conductivity tends not to be an issue due to the good electrical conductivity of the carbon support [4]. However, the same carbon support does not conduct protons well. Consequently, a proton conductive material is added to the carbon support in order to conduct protons to and from the PEM [8].

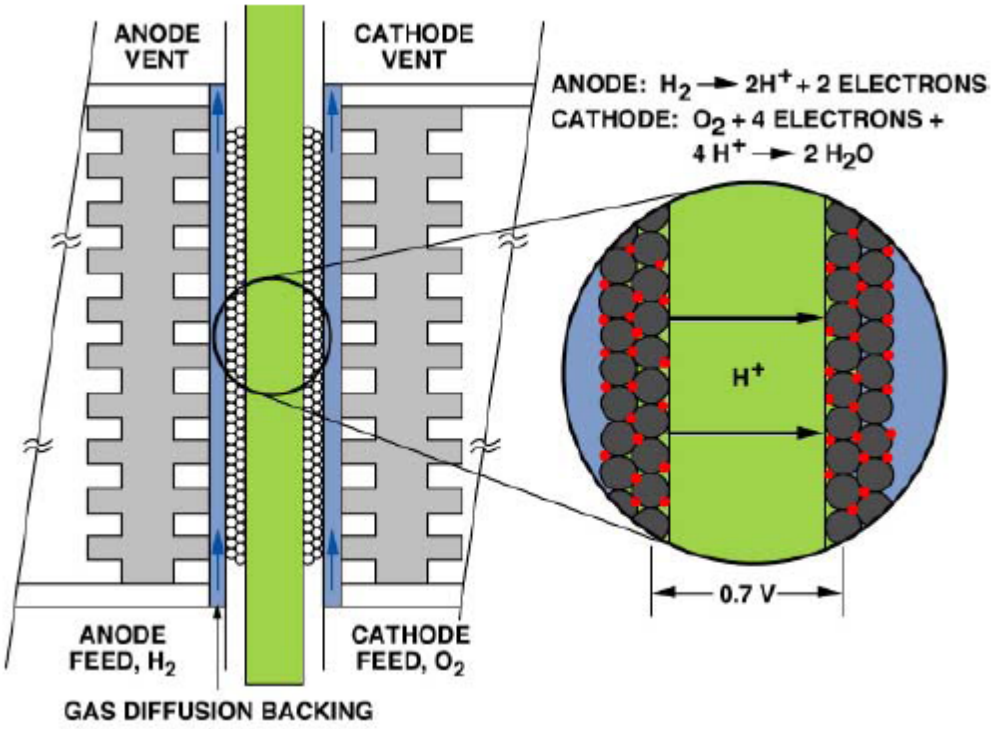

Figure 1. 1: Cross-section of a Proton Exchange Membrane Fuel Cell [6]

1.1.2: Proton Exchange Membranes

The membrane separates the anode and cathode reactions allowing the generation of electricity through the prevention of a direct gaseous reaction [9]. Due to water being

a product in a fuel cell PEMs have to be insoluble in water to be stable for use. Membrane flexibility is important to withstand the pressure exhibited on the membrane during use. The main use of PEMs is to conduct protons across the membrane. Therefore, the ideal PEMs have high proton conductivity yielding faster reaction kinetics and thus higher currents [10]. Membrane conductivity depends on water content as well as the functional groups present within the membrane [11]. The degree of sulphonation (DS) is the percentage of repeated polymer units that contain a sulphonate functional group within the polymer. DS is important to membranes in order for PEMs to be conductive, but high degrees of sulphonation could make the membrane water soluble [12]. Seen in Figure 1.2 is a reaction scheme showing how sulphonate functional groups conducts protons within the membrane with the aid of water. Protons traverse the membrane by transferring between sulphonate groups under aqueous conditions. Various applications for fuel cells require this system to operate under several temperatures and humidities [12-15]. To summarize, general operational criteria for these membranes include: low gas permeability, water insolubility, mechanical flexibility, high proton conductivity and operate under wide temperature/ humidity ranges.

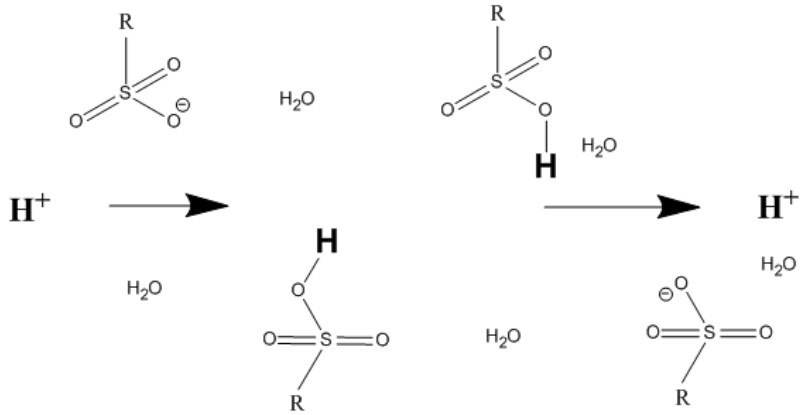

Figure 1. 2: Diagram on Transport of Protons through a Fully Hydrated PEM

1.1.2.1: Nafion

A widely used PEM is Nafion due to its high durability, chemical inertness, water insolubility and high proton conductivity [15]. However, Nafion is expensive ($700 per square meter) and operates ≤ 80˚C due to water loss at higher temperatures and low relative humidity resulting in lower proton conductivity [16]. Nafion has an approximate value of 10% DS that changes depending on the membrane that is obtained. The structure of Nafion is depicted in Figure 1.3 [17]. Nafion has its own distinctive nomenclature that is displayed by AAB configuration. The first two numbers designate the equivalent weight (EW) and the last number in Nafion's nomenclature portrays the thickness in mils (1mil =25.4μm). For example, Nafion 112 has an 1100 EW and is 2 mils thick (50.8 μm), which is commonly used.

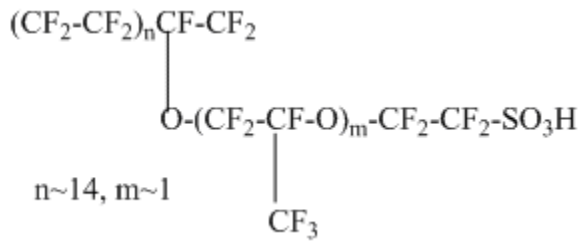

Figure 1. 3: Structure of Nafion

1.1.2.2: Composites

Nafion loses water content in high temperature and in dry conditions resulting in a decrease of proton conductivity [18]. Composite materials consist of two or more different materials combined as one in a specific experimental method. For composite membranes, Nafion is combined with other inorganic or organic molecules in order to improve Nafion's properties. With silica being hydroscopic, it has the potential to

maintain water content within Nafion under dry conditions. Using Nafion in its acidic form, the composite can be made in one step as the precursor is inserted into the Nafion's pores. Previous studies have investigated composites with SiO_2 and Nafion which are promising candidates for maintaining water content in Nafion, however, does not improve proton conductivity [19-21]. Sulphonated silica (SS) is another approach to maintaining water and improves proton conductivity. One example in the literature is using a precursor that has a thiol group and converts to a sulphonate group with H_2O_2 [21-23]. This procedure involves two steps, which is less ideal than a one step synthesis method for a protected monomer. For this thesis the precursor that is used contains a functional group that converts into sulphonic acid in the presence of acid.

1.1.2.3: Purely Siloxane-based

Primarily due to the high cost of Nafion, alternative membrane materials are highly desirable. Sulphonated polysiloxanes have the potential for high proton conductivity at a wider range of temperatures and relative humidity than Nafion [24]. Also, sulphonated polysiloxanes are considerably cheaper due to the precursor and synthesis conditions compared to Nafion which cannot be up scaled due to its fluorine chemistry [17, 25]. Sulphonated polysiloxanes can be made with a sol gel synthesis that is conducted at low temperatures.

1.2: Sol Gel Synthesis

The first step consists of colloidal suspended particles in a liquid phase in a sol gel synthesis and with the proper reaction conditions becomes a polymer network seen in Figure 1.4 [24]. As shown by the detailed reaction scheme in Figure 1.5, the siloxane

monomers are introduced to water and undergo a hydrolysis reaction to form two silica alcohols [26]. Following hydrolysis, the two silica alcohols react together through a condensation reaction to construct the polymer in a Si-O-Si bond formation [27]. This process has its advantages and disadvantages due to the numerous parameters that can be varied to produce membranes with different characteristics.

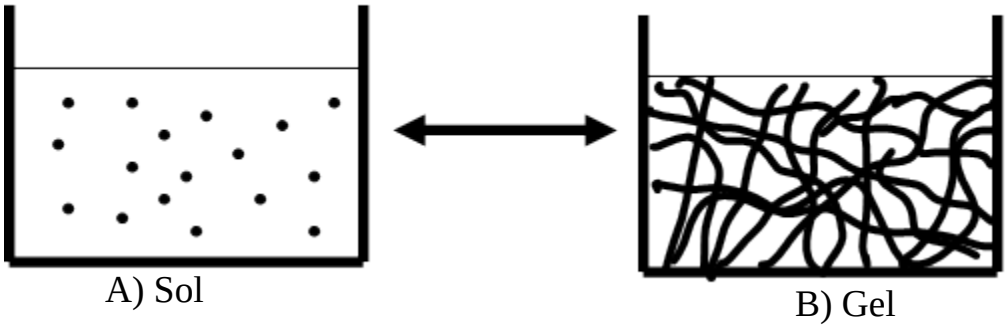

Figure 1. 4: A) Suspended Colloidal Particles (Sol) B) 3D Colloidal Polymer Network

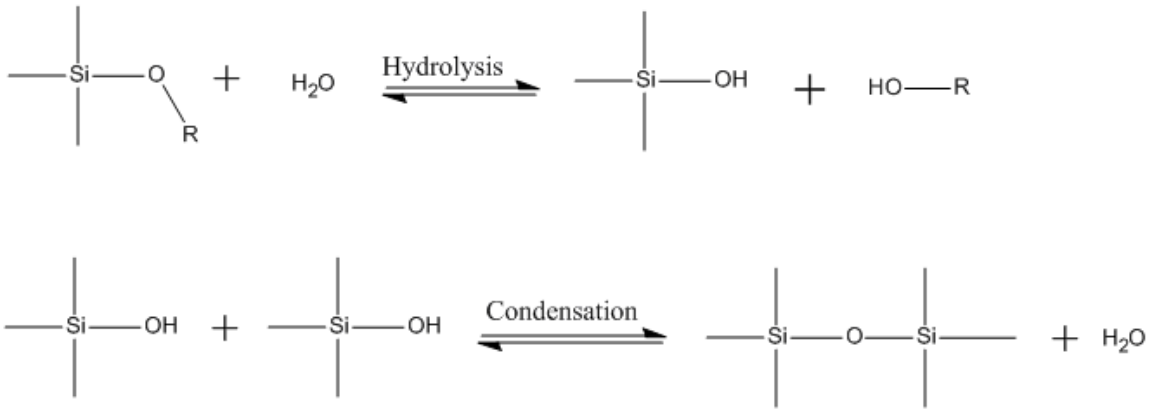

Figure 1. 5: Reaction Scheme for Sol Gel Reactions with Siloxanes

1.2.1: Catalyst

Completion of hydrolysis is rapid only with use of a catalyst [27]. Acid or base catalysis can be used resulting in different basic polymer structures. Reactions with

acidic catalysts result in materials that have linear chains as seen in Figure 1.6A. Basic catalyst produces materials with highly branched clusters shown in Figure 1.6B. These different structures are formed because of the interactions of the protons and the hydroxyl ions on the monomers and its intermediates [28]. Reaction rates of hydrolysis and condensation are controlled by the intermediate steps formed with either acidic or basic conditions. Thus pH can be used to control morphology.

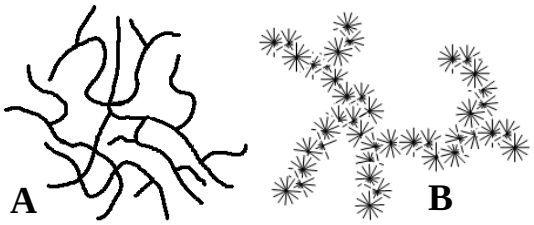

Figure 1. 6: A) Polymer Structure under Acidic Reaction Conditions B) Membrane Structure under Basic Conditions

1.2.2: Water Ratio

The rate of hydrolysis is promoted by water in the system, therefore relative amounts of water and silane are used to control polymerization [27]. Low water to silica ratios result in incomplete polymerization leaving un-hydrolyzed material behind. Consequently, using higher water to silica ratios can promote hydrolysis reactions to completion. From the reaction schemes in Figure 1.5 the hydrolysis reaction is an equilibrium therefore having too much water could have a negative effect by driving the reaction backwards [29]. Therefore, an ideal balance must be determined in order to obtain an adequate level of hydrolysis.

1.2.3: Sterics and Concentration

Functional groups have a role in hydrolysis and condensation reactions therefore having an effect on polymerization. Bulky functional groups can hinder polymerization steps by blocking other monomers from reacting with each other causing incomplete polymerization [30]. Having small functional groups can increase hydrolysis by causing increased collisions with the reactive site of the polymer. If the desired monomer contains a bulky functional group increases in concentration would be ideal to obtain completion of polymerization to have sufficient collisions from having less access to its reaction site.

1.2.4: Solvent and Temperature

Appropriate solvent choice is needed when polymerizing siloxane materials due to various factors. The solvent chosen should not be able to bind with a hydroxyl group due to the resulting decrease in the activity of the solvent [30]. Another crucial property that the right solvent influences is the reaction. Having a solvent for use at low reaction conditions (~60˚C or below) will have fewer molecular collisions to construct the polymer. This can be ideal for the type of polymer needed but in some cases can have unreacted monomers still present after the reaction. On the other hand using solvents with the ability to access at higher reaction temperatures can cause the polymer to have long chains that can entangle within themselves resulting in structures that are flexible and mostly insoluble in various solvents [30]. However when a high degree of chain entanglement occurs, the tangled chains can form knots forming highly rigid structures.

For the particular systems ideal solvent choice is needed to obtain a proper balance in chain length in order to maintain flexible, insoluble polymers [30].

1.2.5: Gellation

Gellation is a process where additional covalent bonds are formed within a polymer system. It occurs when polymers condense to form linkages between clusters of polymer chains resulting in a single cluster [29]. When large, single clusters become to form a highly viscous gel results in gellation [29-31]. On a molecular level the solution fully gels after the last link between the last two clusters has formed [27]. This transition can be noted experimentally by observing sudden increase in viscosity.

1.2.6: Crosslinking

Another consideration that is necessary to consider is the amount of crosslinking that occurs in the resultant membrane. Crosslinking is a covalent bond formed between 2 or more polymer chains creating a branched structure. Figure 1.7A depicts a monomer with three sites able to bind with another monomer resulting in a highly crosslinked membrane whereas Figure 1.7B portrays a monomer with two sites, linear chains and no crosslinking results. A highly crosslinked membrane may not readily dissolve in water due to the higher membrane density [30]. Also, with a high degree of crosslinking the thermal stability increases due to more bonds within the system. However, even though crosslinking solves some issues of membrane stability by increasing water insolubility and thermal stability, the membranes can become very rigid and inflexible [27]. While limiting potential crosslinking aids in membrane flexibility, long linear chains introduce chain entanglement which is equally problematic [30]. Another property that membranes

can process is the ability to swell that commences with the membrane being able to absorb water into the membrane. When membranes swell, the mechanical properties of the membrane become weaker as the membrane expands. The amount of swelling can be controlled by the amount of crosslinking. Consequently, it is important to moderate the degree of crosslinking in order to obtain ideal membranes.

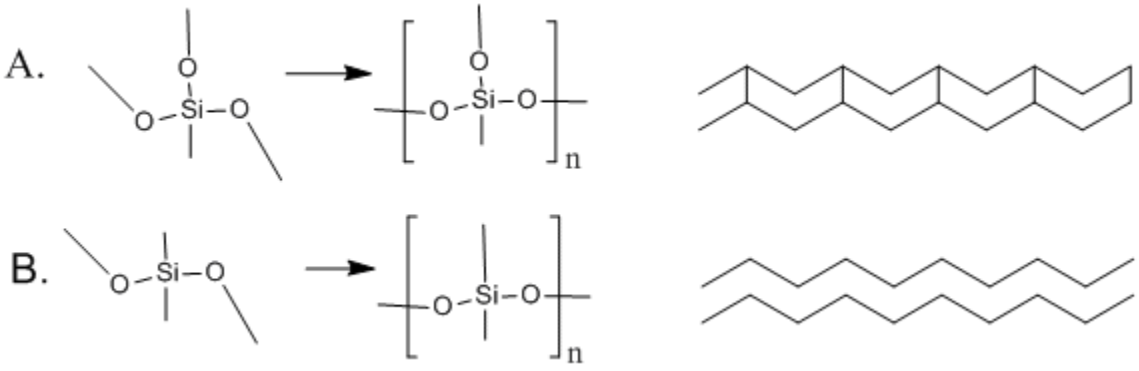

Figure 1. 7: Crosslinking Diagram for Siloxane Polymerization A) High Crosslinkng B) Low Crosslinking

1.3: Water and Membranes

Polymer interactions with water need to be determined because fuel cell operation produces water as a product and membranes need water to conduct protons. An issue with water is product solubility and swelling, both of which are dependent on the membrane's ability to uptake water. Swelling of the membrane results in the structure becoming mechanically fragile within the fuel cell and becoming less proton conductive. Figure 1.8 depicts various interactions of membranes with water. Figure 1.8A is when a membrane is considered dry with the colloidal particles suspended within the membrane system being not proton conductive. With the addition of water the colloidal particles

swell (Figure 1.8B) and if the membrane can uptake more water then swelling colloidal particles connect which allows protons to transverse through the membrane, which is the state where ideal proton conductivity occurs (Figure 1.8C). If the membrane contains more water a structural inversion occurs on the connected colloidal system (Figure 1.8D). Figure 1.8E and 1.8F depict membranes that can absorb excess amounts of water that result in its dissolution.

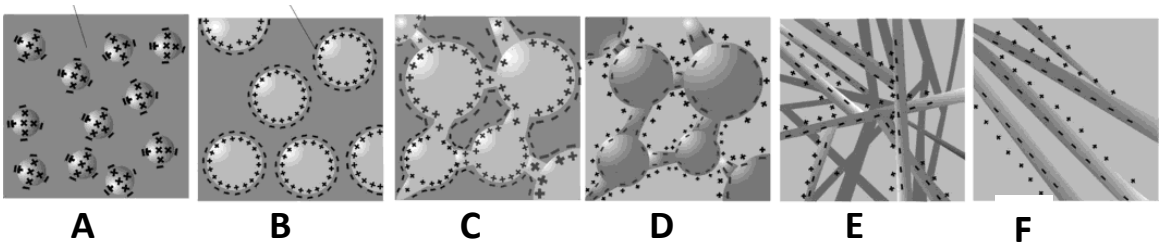

Figure 1. 8: Membrane Behaviour in Various amounts of Water A) Dry Polymer B) Swelled Clusters C) Percolation D) Charge Inversion E) Suspension of Colloidal Rods F) Dissolution [17]

1.4: Electrochemical Impedance Spectroscopy (EIS)

To determine a membrane's conductivity electrochemical impedance spectroscopy is employed. In electrical circuits resistance is determined by Ohm's law in a DC system (Equation 1.3). The resistance obtained from this equation is based on ideal systems. With an ideal resistor (R) the potential (V) and current (I) signals are in phase with each other meaning the responses are directly proportional.

$$I = \frac{V}{R}$$

Equation 1.3

In an AC system the capacitor creates a phase shift between the potential and current responses shown in Figure 1.9 [32]. The potential and current signals can then be

expressed as mathematical function with the response of a sine wave (Equation 1.4 and 1.5) [5]. With the responses known for the potential and current, these equations can be related to Ohm's law with impedance in place of resistance to form the impedance response of this system seen in Equation 1.6. Like resistance, impedance is the ability to impede electric current.

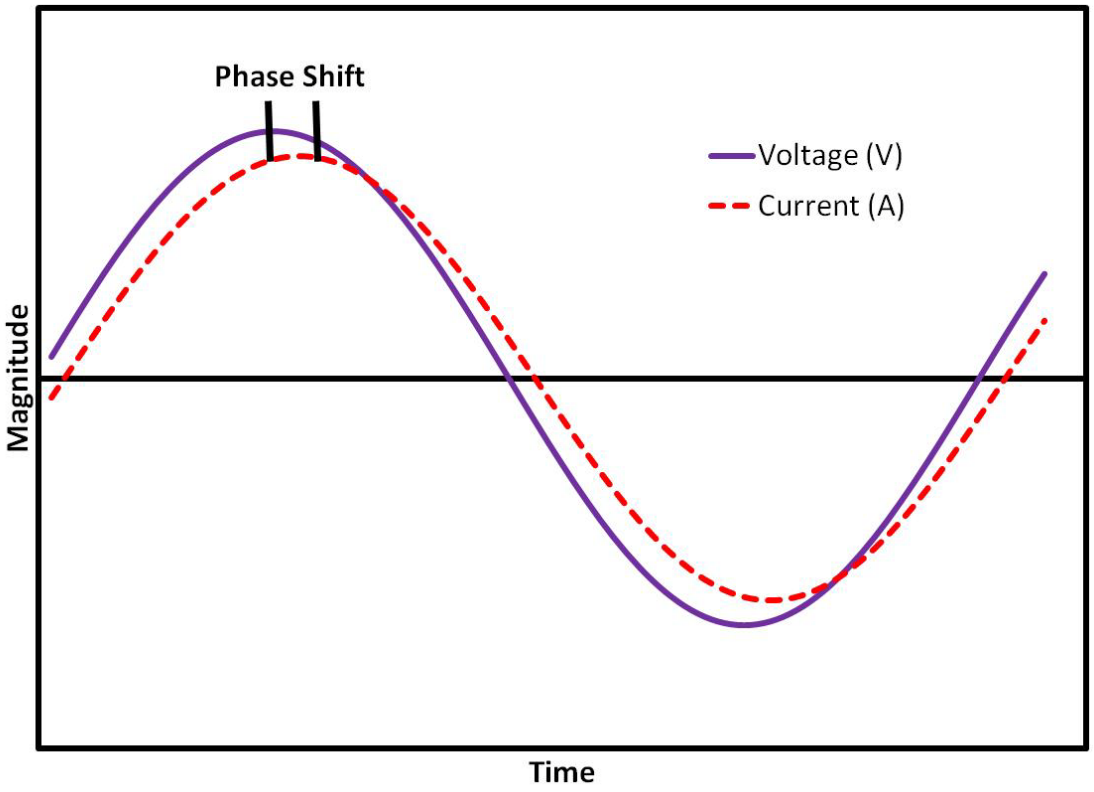

Figure 1. 9: Relationship of Current and Voltage Response for Real Electrical Systems

$$V = V_0 \sin(\omega t) \qquad \textbf{Equation 1.4}$$

$$I = I_0 \sin(\omega t + \Phi) \qquad \textbf{Equation 1.5}$$

$$Z = \frac{V}{I} = \frac{V_0 \sin(\omega t)}{I_0 \sin(\omega t + \Phi)} = Z_o \frac{\sin(\omega t)}{\sin(\omega t + \Phi)}$$

Equation 1.6

With Eulers identity, the impedance response can be written as a complex function that can be seen in Equation 1.7. The impedance can be plotted in a Cartesian plane, called a Nyquit plot, where the x axis is the resistance in Ωcm^2 denoted as Z' and the negative y axis is due to the capacitance denoted as Z" [33]. Figure 1.10 depicts a typical Nyquist plot that is plotted from high frequency to low frequency and shows the circuit that represents this system. In electrochemical impedance spectroscopy an electrical circuit is used to explain the chemical system. The circuit contains two resistors where one represents the resistance of the cell (R_c) and the other resistance is associated to the membrane (R_m) [34]. The capacitor portrays the interface that occurs between the membrane and the electrode, where positive charges are stored on one side and negative charges are stored on the other. When frequency is high, the electrons travel through the path of least resistance, which is the capacitor. The capacitor exhibits more resistance as the frequency decreases.

$$Z = \frac{V}{I} = Z_o(\cos\Phi + j\sin\Phi) \qquad \textbf{Equation 1.7}$$

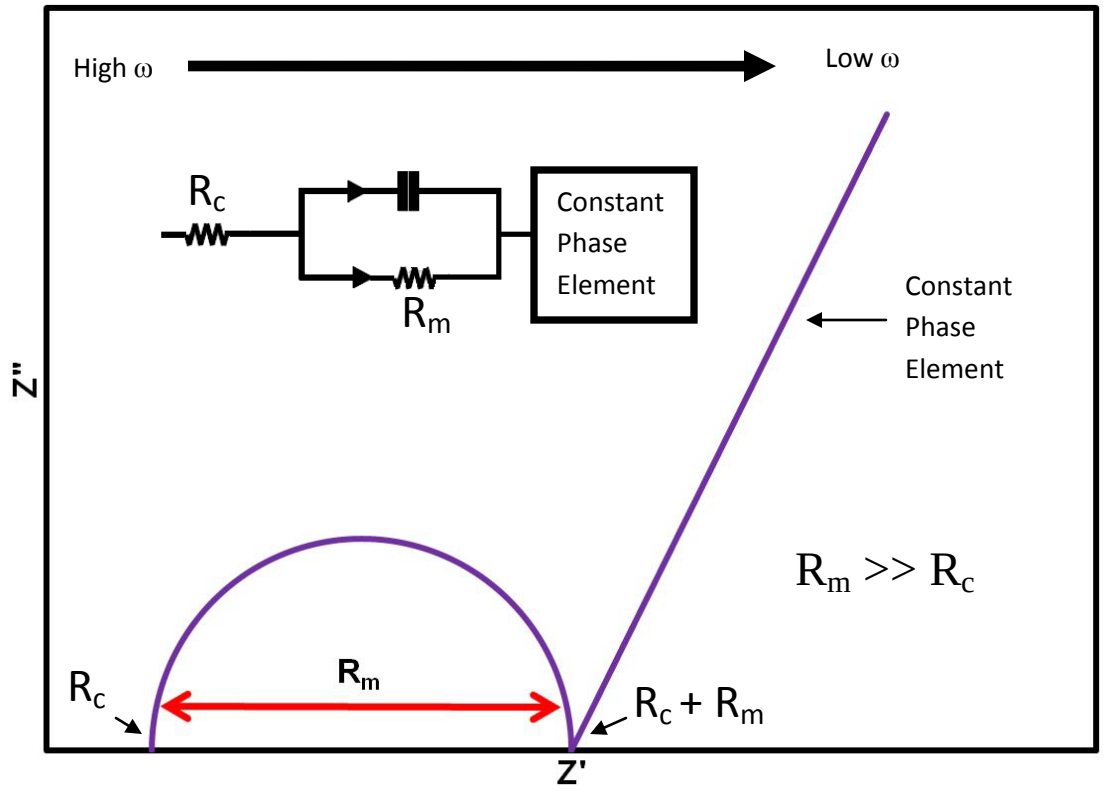

Figure 1. 10: Typical Nyquist Plot Response for an AC Impedance System

1.5: Thesis Objective

The goal of this research was to synthesize a proton exchange membrane for fuel cell applications by either polymerizing new materials, such as polysiloxanes, or to improve existing materials like Nafion through composites.

Synthesizing new materials from sulphonated silanes was performed through sol gel procedure at high pH to obtain ideal membranes. The sol gel procedure had to be optimized for the precursors used, therefore numerous parameters were varied to determine the ideal method for producing PEMs.

Composite membranes were made with sulphonated silica materials to target water retention in dry conditions and to improve proton conductivity. An adaptation on a procedure was used in synthesizing composite membranes; however this had to be altered due to sulphonated silane composition.

Various characterization methods including water solubility, thermogravimetric analysis (TGA), fourier transform infrared spectroscopy (FT-IR), proton conductivity by electrochemical impedance spectroscopy (EIS) and fuel cell testing were used to determine product suitability for PEM fuel cell applications.

Chapter 2
Materials and Methods

2.1: Sol Gel Synthesis

A synthetic scheme shown in Figure 2.1 depicts the overall steps involved in a sol gel synthesis to produce free standing membranes. For a sol gel synthesis different combinations of monomers were used as portrayed in Table 3.1 to produce varied morphologies to obtain an ideal PEM. Methanol, ammonia hydroxide and water were placed with the monomers in a one pot synthesis method. The colloidal suspension was refluxed for six hours and was casted by different methods described below. Parameters were optimized to obtain the ideal membrane for a fuel cell, therefore amounts of water, methanol, degree of sulphonation, and ratio of precursors were changed throughout this investigation.

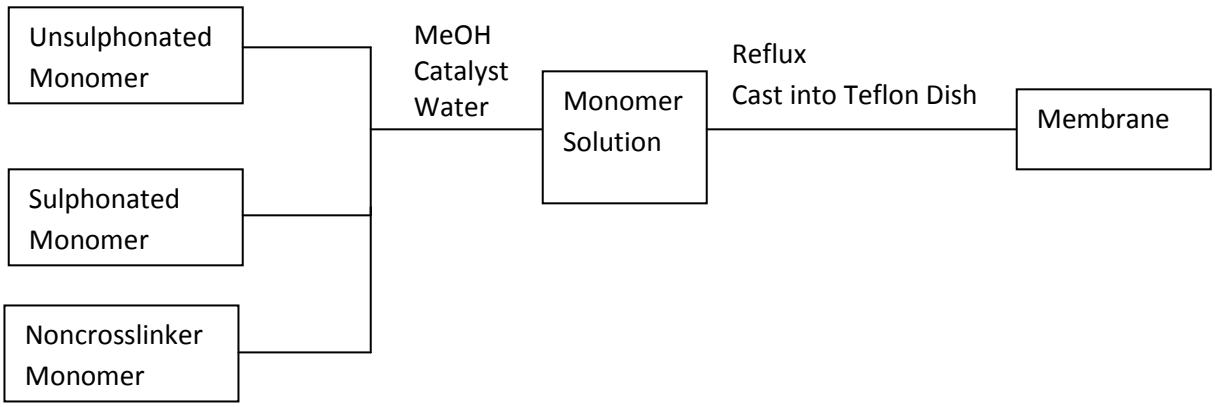

Figure 2. 1: Reaction Scheme to Produce Polysiloxane Proton Exchange Membranes

2.1.1: Monomers Specifications

The sulphonated monomer used was 2(4chlorosulphonylphenyl)ethyltrimethoxysilane (CSPETMOS) used as received from united chemical technology or 3-(trihydroysilyl)-1-propanesulfonic acid (TPS) used as

received from Gelest, and the unsulphonated precursor was phenethyltrimethoxysilane (PETMOS) used as received from Gelest (Figure 2.2). Dimethyldimethoxysilane (DMDMOS) was the monomer to limit crosslinking used as received from Sigma Adrich (Figure 2.2). Membranes synthesized initially were 100% DS in which only the monomer CSPETMOS was used. Copolymers were made with CSPETMOS and PETMOS as well as copolymers with CSPETMOS, PETMOS and DMDMOS. An investigation of monomers used for sulphonation occurred that used TPS instead of CSPETMOS. When the above monomers polymerize they form sulphonatedpolyphenylethylsilane (SPPES). For reference, membrane codes will be presented as SPPES with a number present afterwards to distinguish between the compositions of each membrane. The solvents used were methanol (Fisher) and ethylene glycol (Sigma Aldrich) and the catalyst used was 6M ammonia hydroxide (Sigma Aldrich). Figure 2.3 depicts an example reaction scheme of CSPETMOS, PETMOS and DMDMOS added at various molar ratios.

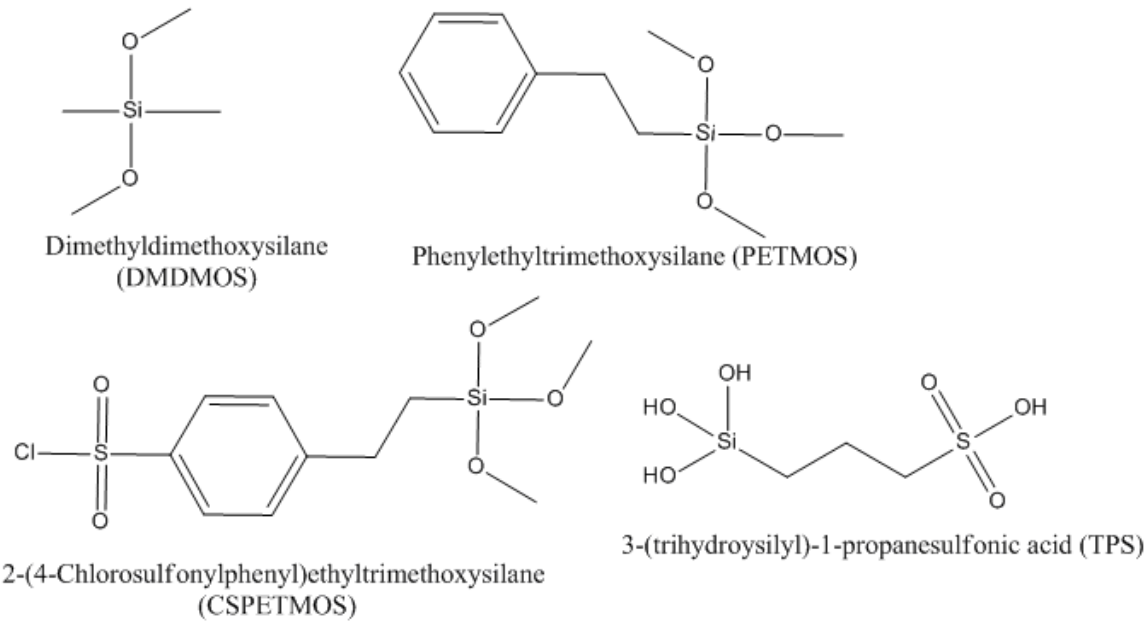

Figure 2. 2: Precursors used in Synthesis of PEMs

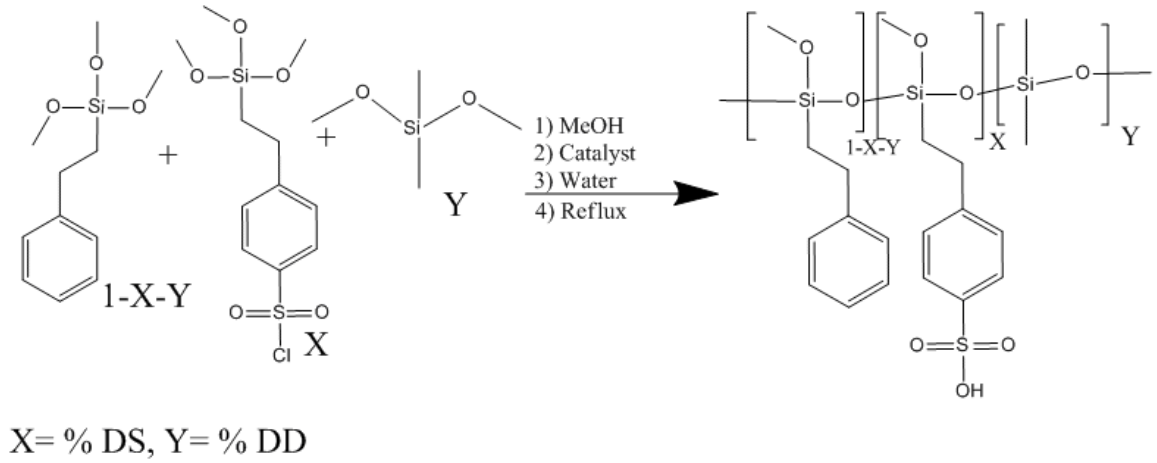

Figure 2. 3: Polymer Synthesis and Structure of Copolymer made with CSPETMOS, PETMOS and DMDMOS

2.1.2: Casting Methods

2.1.2.1: Liquid Product cast into Dish

After reflux the resultant liquid was poured into a Teflon dish for the solvent to evaporate. With this method condensation and gellation reactions happen in the dish simuteously. The time allowance for both processes was dependant on the time for the solvent to fully evaporate. For some membranes the time that was allowed for both processes of condensation and gellation was not enough resulting in unreacted monomers. Therefore another method was employed.

2.1.2.2: Casting Pre-gelled Product

Another method was to gel samples to promote longer chain growth by containing the solvent within the system for a longer period of time. Exposing the system to air caused moisture to be introduced at a slower rate to promote additional chain growth. This was done by stirring the solution in its reaction vessel (3 neck flask) while exposed to air for the solvent to evaporate for a longer duration. Solutions were stirred until their

viscosity suddenly increased. Viscosity was a simple method in observing if the product has undergone gellation. The gelled product was placed on either a Teflon or a polystyrene covered surface for easier recovery. Using a polystyrene surface prevented the product from bonding to the glass surface that would result in damages to the membrane during recovery. To retrieve a membrane from a polystyrene covered surface, the polystyrene layer was dissolved using a solvent that would dissolve the polystyrene layer but not the gelled product such as chloroform or dichloromethane (Figure 2.4) [31].

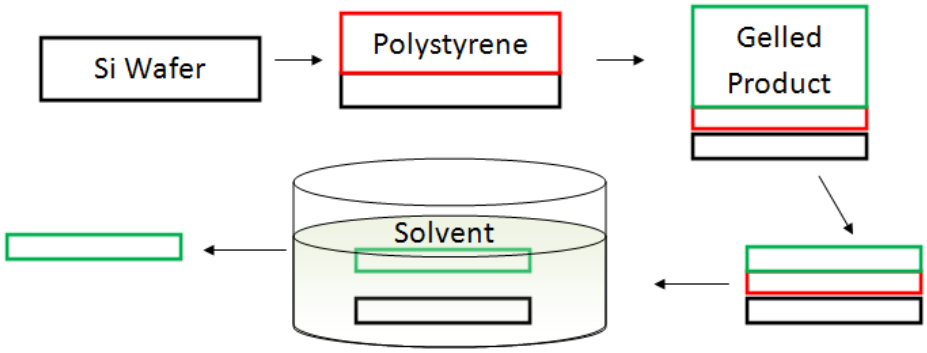

Figure 2. 4: Recovery of Gelled Product from Polystyrene slides

2.2: Composite Synthesis

This procedure was an adaptation from Jung et al. and is depicted in Figure 2.5 (19). The silanes used were either tetraethylorthosilicate TEOS (Sigma Aldrich) or CSPE. For composite membranes Nafion (Dupont) must be cleaned initially to remove impurities. Elimination of impurities was performed through a series of boiling solutions of DI water, 3% H_2O_2, DI water, 0.5M H_2SO_4 and DI water [19]. All reagents were from Sigma Aldrich and used as received. The cleaned Nafion was swelled in a 4:1 ratio of methanol to water for 24 hours. Swelled Nafion was then immersed into a solution that

contained methanol and silane material. The methanol and silane were stirred for 3 hours in varied ratios. Composite silica loadings were controlled by varying the impregnation time as well as the concentration of the silane solution. The obtained composite membrane was then placed on a Petri dish and heated in an oven for 24 hours. The composite was recovered by swelling the product with water to remove it from the glass.

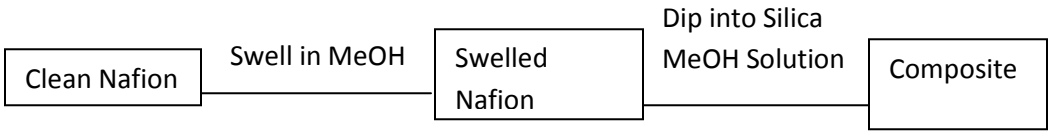

Figure 2. 5: Synthetic Scheme for producing Composite Membranes [18]

2.3: Membrane Characterization

2.3.1: Solubility Tests

Determination of membrane solubility was performed by placing a small piece of membrane in deionized water to observe the behaviour of the product over time. From this test membranes were labelled as soluble or insoluble. For samples that were insoluble in water, the amount of swelling that occurred was observed. These vials were kept to observe swelling properties over long periods of time, as a qualitative method .

2.3.2: Thermogravimetric Analysis (TGA)

TGA was performed on a TA Instruments SDTQ600 Thermal Analyzer. This technique was used to study the decomposition or combustion of product membranes. Decomposition studies were performed by exposing the membranes to argon and raising the temperature by 20°C/min from room temperature to 1000°C. Combustion analysis

was done similar to the decomposition study with samples exposed to dry air instead of argon. All samples are placed into an alumina pan with no additional sample preparation required.

2.3.3: Infrared Spectroscopy

Membranes that are intact or in the form of powders can be analysed on a Nicolet 4700 Fourier Transform Infrared (FT-IR) spectrometer using ATR. Samples were placed on a zinc selinide (ZnSe) flat plate which is tilted at an angle of 45˚. If membrane was intact it was placed directly on the crystal for analysis. For samples that were not intact were grounded into a finer powder prior to placement directly on the crystal. Full membrane samples were placed directly on the ZnSe plate.

2.3.4: Electrochemical Impedance Spectroscopy

Measurements were taken on a Solartron 1470E Multichannel Potentiostat and a 1260 frequency response analyzer for the in-plane conductivity measurements. The frequency range that the readings were taken was from 40 000 to 500. There were two methods used to determine impedance of the membranes. The first was in-plane conductivity and the second was through-plane conductivity. Data was captured with impedance software called Z plot for data analysis. All samples were placed into the cell after being placed in water for twenty four hours.

2.3.4.1: In-Plane Conductivity

Figure 2.5 shows how the membrane is placed into the Teflon cell which has brass contacts. Inside the cell was a membrane with Pt black electrode on both sides.

The contacts for the system are separated only by the membrane, therefore the path of current is small as depicted by the arrow in the membrane (Figure 2.5). By having the contacts so close the current travels through limited material causing very low resistance to be observed. The total resistance is placed in Equation 2.1 to determine the membrane's proton conductivity, where R_m is the membrane resistance, R_c is the resistance of the cell, R is the total resistance, d is thickness of the membrane and σ is the conductivity. This method was ideal because in-plane conductivity measurements were more time efficient and in the same orientation as the fuel cell.

$$R = R_m + R_c = \frac{d}{\sigma} + R_c, where\ \sigma = \frac{d}{R_m} \qquad \textbf{Equation 2. 1}$$

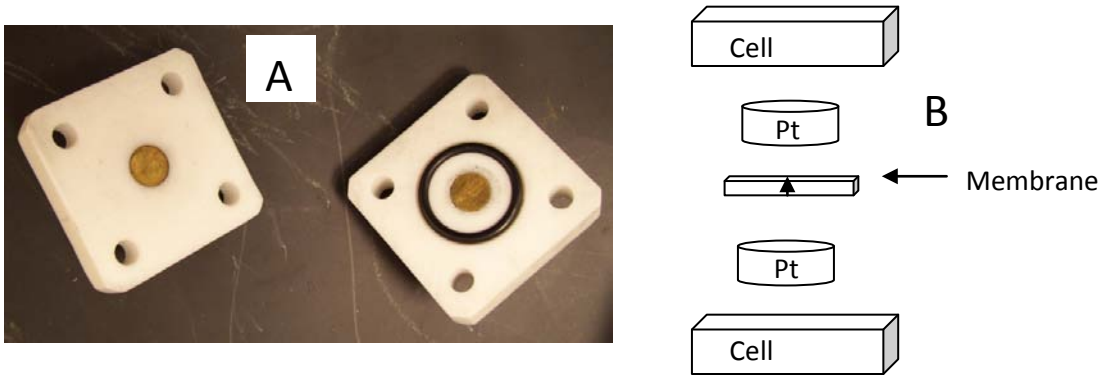

Figure 2. 6: A) In Plane Conductivity Cell B) Arrangement of Cell Constituents

2.3.4.2: Through-Plane Conductivity

Through-plane measurements were taken in standalone mode using the 1260 frequency response analyzer only. The through-plane conductivity cell contains Pt plates that are 1cm apart and there is a window on both sides that are $1cm^2$ to expose the membrane to external conditions (Figure 2.6). Through-plane measurements are more accurate than in-plane; however measurements are not taken in the same orientation as the cell and it takes longer to obtain values (34). Unlike in-plane conductivity, through-

plane conductivity can obtain conductivity values in different conditions with a humidity chamber. Equation 2.2 depicts the relationship used to obtain conductivity value, where L is the length (1cm), A the area of the membrane (Figure 2.6) and R_m the resistance of the membrane.

$$\sigma = \frac{L}{A * R_m}$$

Equation 2. 2

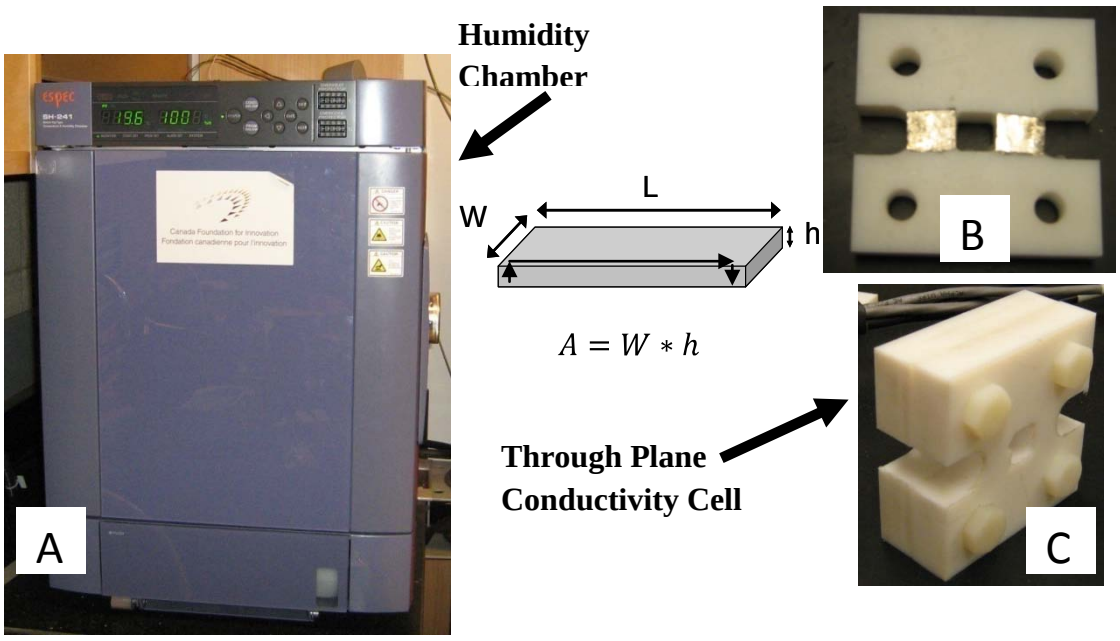

Figure 2. 7: A) Humidity Chamber B) Membrane Geometry C) Humidity Cell

2.3.5: Fuel Cell Testing

Fuel cell measurements are taken by the same orientation as the in-plane conductivity cell as seen in section 2.3.4. Membranes that displayed the best qualities were analysed in a fuel cell. Samples were hot pressed (Figure 2.8) with standard

electrodes that were made with the protocol from Eastcott et al. [8]. The conditions for making the membrane electrode assembly (MEA) in the hot press were 150kg/cm^2 of pressure at 135˚C for 90s (Figure 2.8A). MEAs (Figure 2.8B) were then placed into a fuel cell (Figure 2.8C) that contains a 5cm^2 electrode area. $H_2/O_2/N_2$ were gasses used for the fuel cell are passed through a humidifier before entering the cell, where the relative humidity (RH) was dependent on the temperature as seen in Equation 2.3. The potential and currents that are produced by the cell are recorded in CorrView (electrochemical program) for analysis. P_{H2O} was the partial pressure of water and P^*_{H20} was the saturated vapour pressure of water, which is a function of RH.

$$RH = \frac{P_{H_2O}}{P^*_{H_2O}} * 100\%$$

Equation 2.3

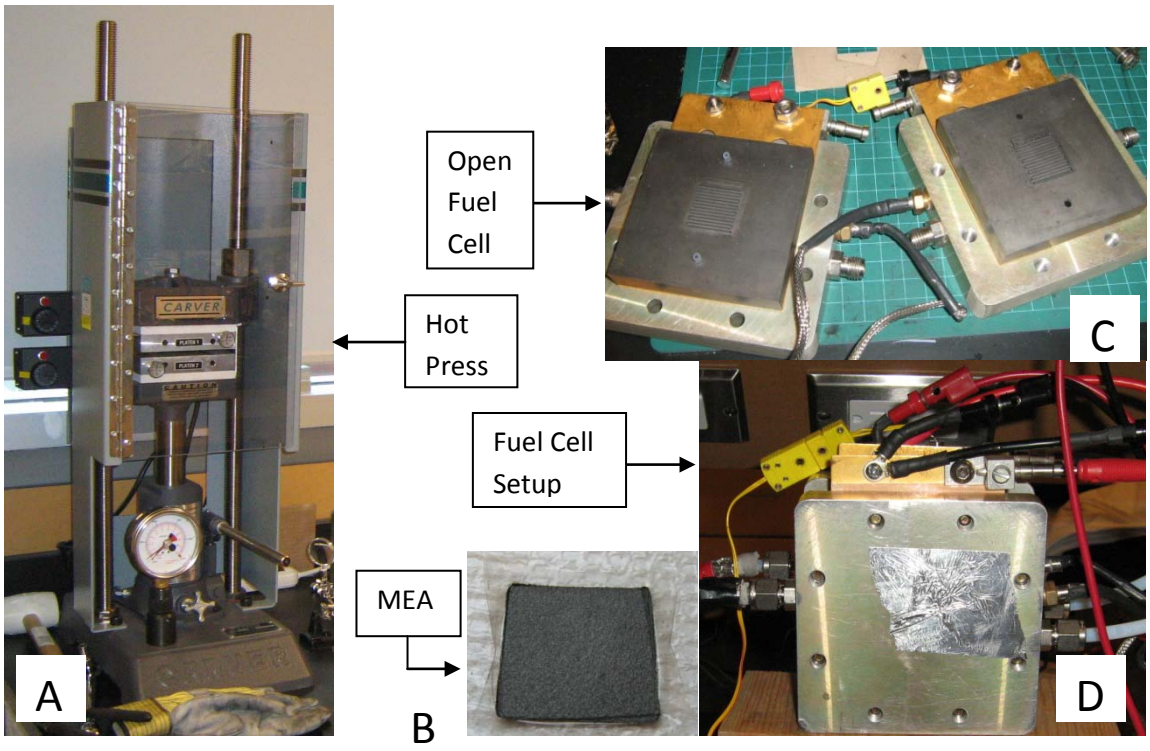

Figure 2. 8: Fuel Cell Testing Set-up and Experiment A) Hot Press B) MEA C) Fuel Cell Open D) Fuel Cell in use

Chapter 3

Sulphonated Polysiloxane

Results and Discussion

3.1: Polysiloxane Membranes

Alternative PEMs are needed to reduce cost in fuel cell operation and to operate at higher temperatures. A method to produce alterative PEMs was performed by synthesizing polysiloxane membranes through a sol gel method that can be controlled by numerous parameters to be able to control the membrane's morphology and properties. Therefore a thorough optimization was conducted to obtain an ideal alternative. The membrane synthesized were sulphonatedpolypheylethylsilane (SPPES). Membrane names and chemical compositions are tabulated in Table 3.1 with its properties. The nomenclature for membranes are SPPES(DS) #, where DS was the amount of sulphonation and # was the membrane code.

3.1.1: Water Ratios

A polymer made from purely 2-4chlorosulphonylphenethyltrimethoxysilane (CPSETMOS) was synthesized using numerous water to silica molar ratios (3:1, 6:1, 9:1 and 12:1) to observe its effects on the membrane (Table 3.1 SPPES 1). The polymer structure is displayed in Figure 3.1. To observe the ideal water ratio would be to determine the amount of polymerization that occurred within the polymers. In TGA curves shown in Figure 3.2 it can be seen that the 3:1 water ratio contained unreacted monomer as shown by the presence of additional peaks in the 100-200˚C range. Resultant membranes were inflexible and hard. The limited water content was not adequate to polymerize all the monomers. TGA curves with absent additional peaks in the 100-200˚C portray full polymerization, which occurred with higher water ratios. The 9:1 and 12:1 water ratios created membranes that broke apart when handling indicating over promotion of hydrolysis. A 6:1 water ratio produced a membrane that was relatively

flexible compared to the others but overall inflexible. Both qualitative observations and the TGA results depict that a 6:1 water ratio is optimal. However all these membranes were soluble in water, therefore being unsuitable for use in a fuel cell therefore additional optimization was required.

3.1.2: Concentration of Monomer

Using SPPES 1 (Figure 3.1) its reaction rates during the sol gel process were controlled by changing reactant concentration. Variable monomer concentrations of CSPETMOS that were investigated were 0.22M, 0.35M, 0.49M and 0.84M. The best concentration was found to be 0.49M due to the membrane exhibiting higher flexibility. Higher concentrations produced hard powders that could not form films. As seen in Figure 3.3 the TGA curves depict membranes with no unreacted monomer. However, even with the gain of higher flexibility the membranes were still soluble in water.

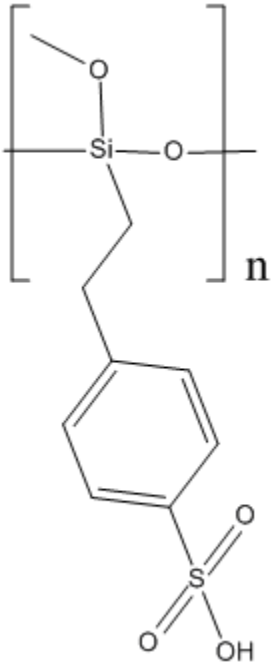

Figure 3. 1: Polymer Structure for the polymerization of SPPES 1

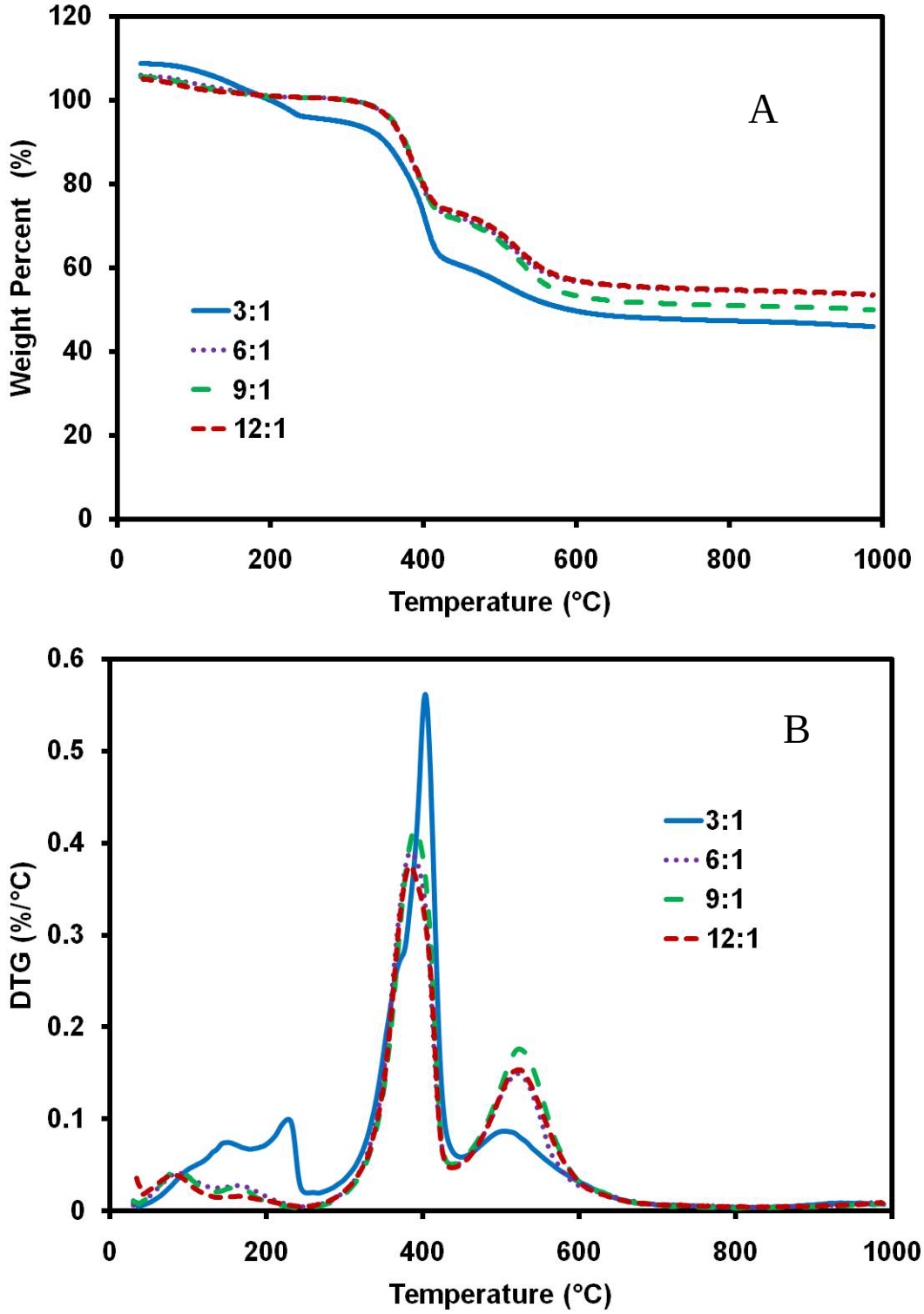

Figure 3. 2: Decomposition of 3:1, 6:1, 9:1 and 12:1 Water to Silica Ratios on SPPES 1 A) Thermograph B) Derivative Thermograph

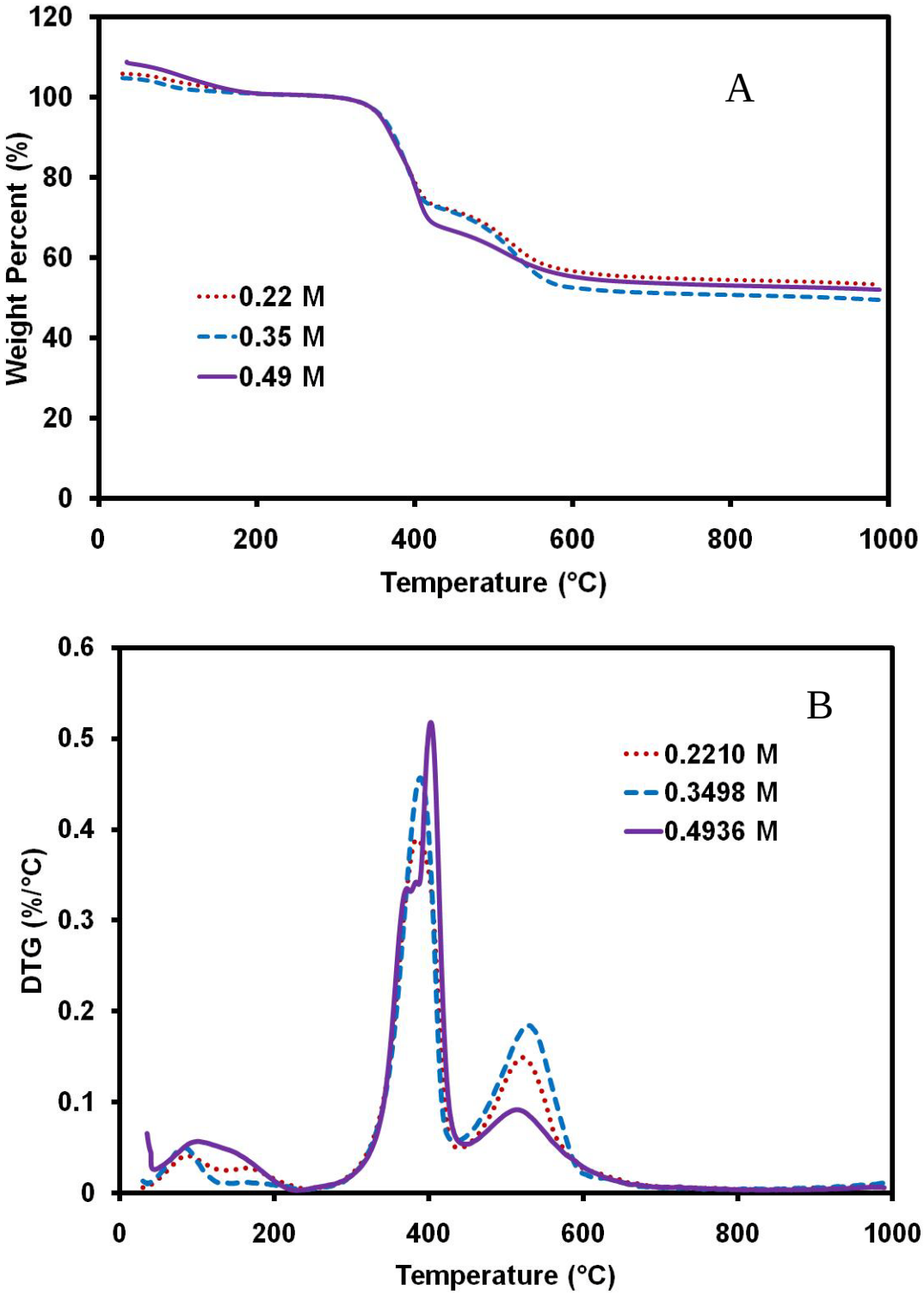

Figure 3. 3: Decomposition of 0.22M, 0.35M and 0.49M Concentration of Monomer on SPPES (100) 2 A) Thermograph B) Derivative Thermograph

3.1.3: Degree of Sulphonation

To obtain insoluble membranes the degree of sulphonation (DS) was changed making a copolymer as shown in Figure 3.4, where DS is X, by using CSPE and phenethyltrimethoxysilane (PE). The sulphonate functional group is hydrophilic causing the observed solubility issues, however lowering the sulphonation results in lower conductivity. Thus a balance is necessary to optimize insolubility and proton conductivity. Lowering the DS made the membranes less soluble, but caused higher inflexibility. SPPES(100) 1, SPPES(80) 2 and SPPES(40) 3 were characterized by TGA portrayed in Figure 3.5A that between 400-500˚C there was less sulphonate functional groups present to determine DS. This is also confirmed with the DTG curve (Figure 3.5B) in the 350- 450˚C range showing peak height decreases as membrane DS decreases. Additional conformation was determined by FTIR that depicts sulphate stretches at 1080 and 1018cm^{-1} (Figure 3.6) (35). Solubility tests demonstrated membrane were completely insoluble at < 20% DS. Further decreases in sulphonation would result in membranes with lower conductivity. Therefore the higher DS that can be obtain while maintaining insolubility would be ideal. Optimal DS was found to be approximately 20% however it was still relatively inflexible.

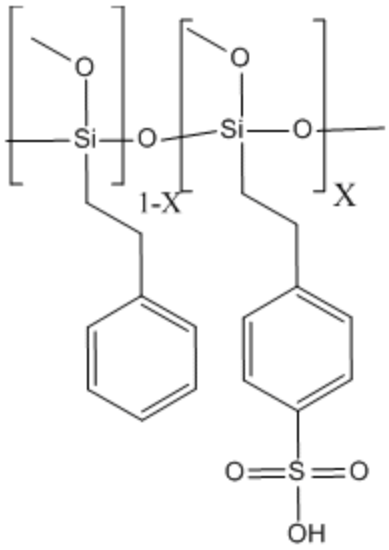

Figure 3. 4: Copolymer Structure for CSPETMOS and PETMOS, where X is the Degree of Sulphonation

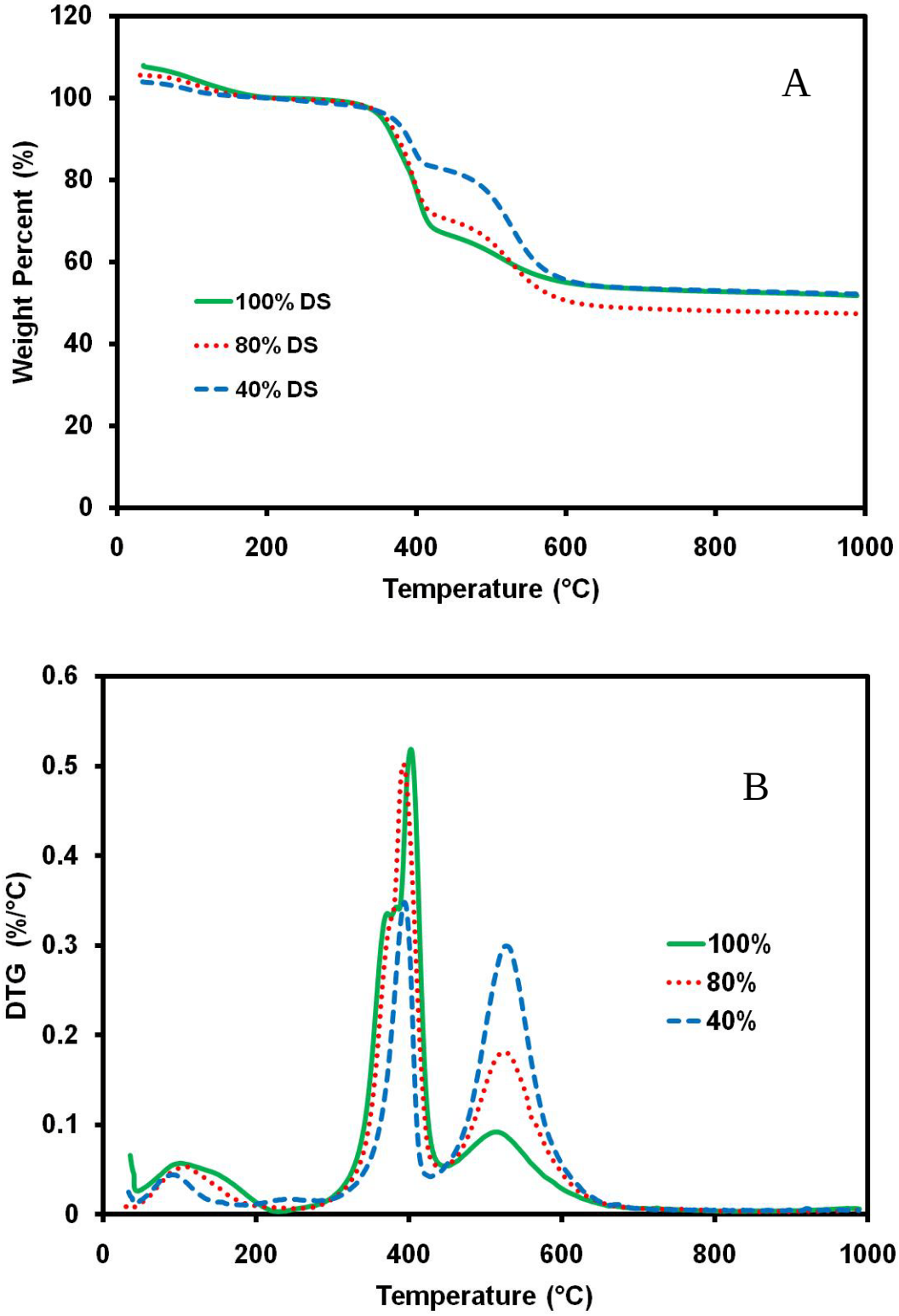

Figure 3. 5: Decomposition of 100% DS, 80%DS and 40% DS A) Thermograph B) Derivative Thermograph

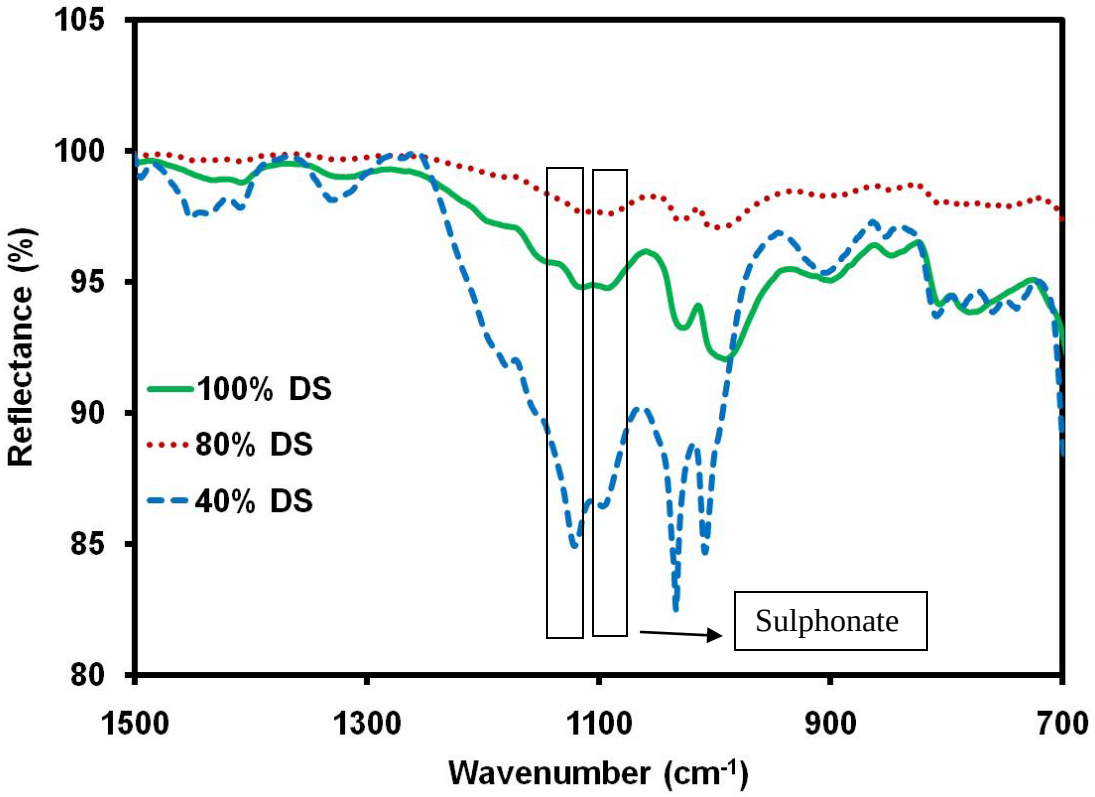

Figure 3. 6: Infrared Spectrum of Various Degree of Sulphonation on SPPES(100) 1, SPPES (80) 2 and SPPES (40) 3

3.1.4: Solvent and Temperature

One method that can aid in increasing membrane flexibility and to maintain insolubility is by varying reflux temperatures. Higher temperatures promote longer chain lengths, resulting in flexible and durable products. Chain entanglement can also produce knots which contribute to membrane insolubility in various solvents. Lowering the reflux temperature caused membranes to become brittle and the TGA curve shown in Figure 3.7 demonstrated that there was unreacted monomer as well. Membranes refluxed at 60˚C indicated larger extent of polymer chains seen in Figure 3.7. To perform reactions at temperatures higher than 60˚C a substitute for methanol had to be found. Ethylene glycol was used to raise the reflux temperature to 100˚C. The membranes produced were highly

flexible and exhibited adhesive properties. Figure 3.7 depicts a large amount of additional peaks. There are two possible explanations for the additional peaks in the TGA. Ethylene glycol is a diol and thus the first possibility is that it may participate in the condensation reaction, effectively, inserting poly ethylene glycol linkages into the backbone of the polymer, as depicted in Figure 3.7. This is supported by the work of Yang et al. who employed ethylene glycol to limit the amount of crosslinking in polyimides, thereby producing more flexible membranes [36]. These membranes were prepared under similar reaction temperatures and conditions to that reported here. The second possibility is that ethylene glycol can be trapped within the pores and act as a plasticizer. The latter possibility is the most likely, though we cannot rule out some contribution from the former. Regardless, this clearly illustrates that ethylene glycol was not a good choice in synthesizing PEMs.

3.1.5: Summary of Optimization

Promotion of hydrolysis was maintained by using a 6:1 molar ratio to produce membranes with fully reacted monomer. However the concentration was not too high as to overpromote hydrolysis at the expense of condensation. Concentration of monomer was manipulated to influence reaction conditions resulting in more flexible membranes. This was achieved by using a 0.49M monomer concentration. Also, ethylene glycol polymerized itself and stayed in the pores of the membrane making them unstable in water. A 20% DS was used since it did not readily dissolve in water. To summarize, the optimized procedure used was a 6:1 water ratio, 0.49M monomer concentration, methanol solvent and 20% DS. These conditions produced membranes that were insoluble in water though relatively brittle.

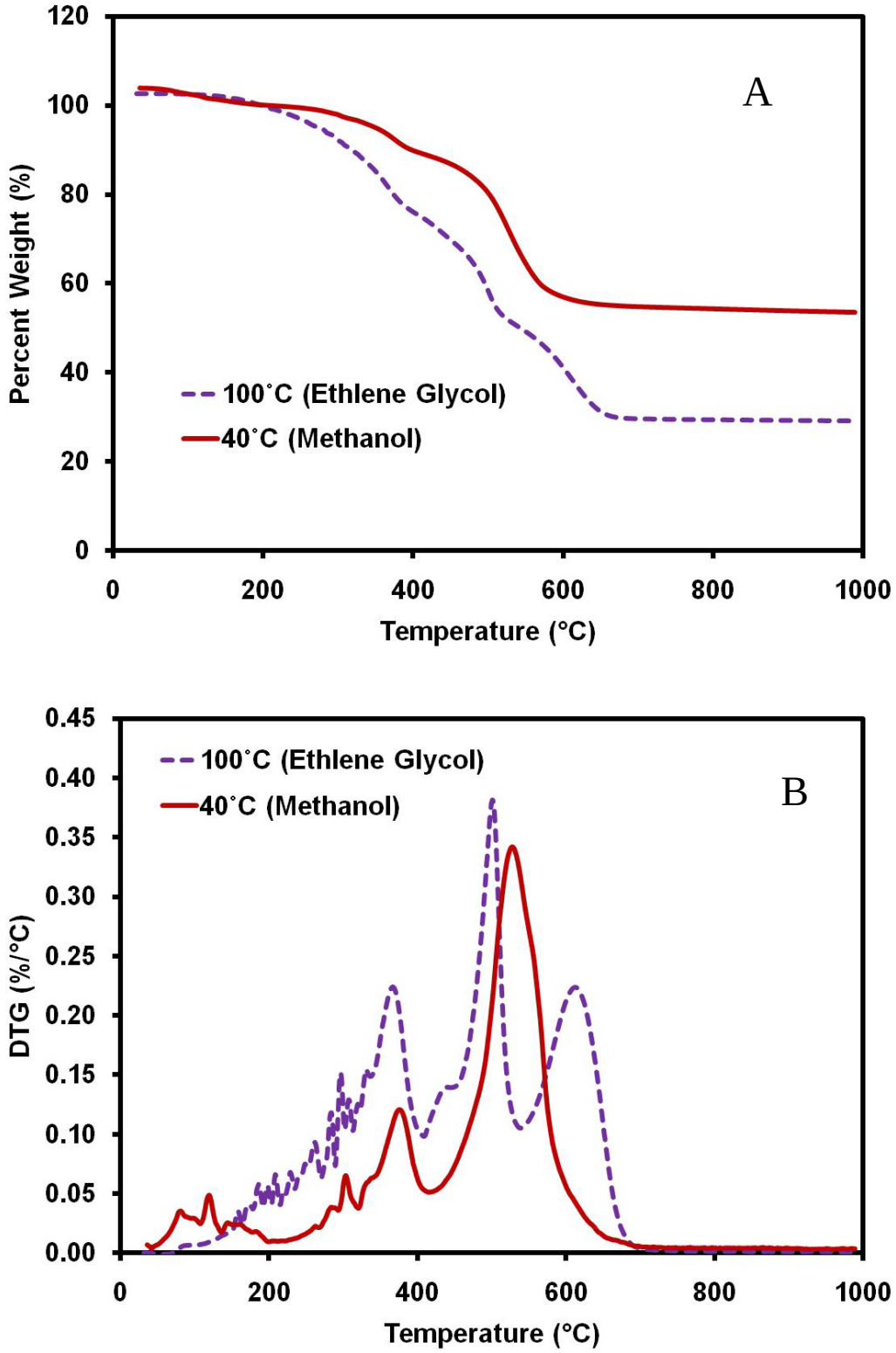

Figure 3. 7: Effect of Solvent and Temperature Refluxes in Ethylene Glycol (100˚C) and Methanol (60˚C) using SPPES(20) 4 under Argon to Observe Decomposition A) Thermograph B) Derivative Thermograph

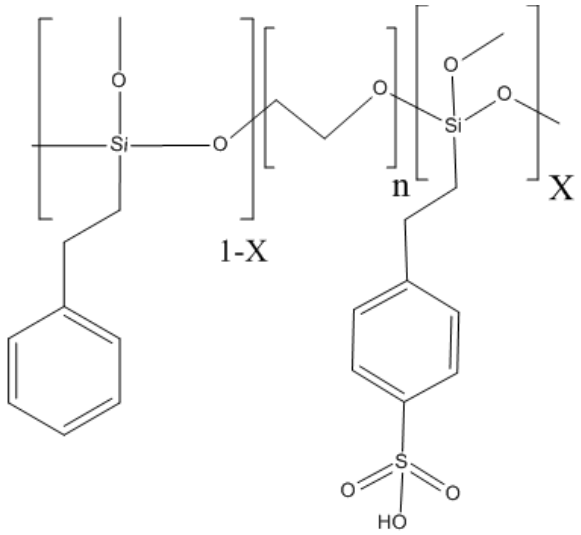

Figure 3. 8: Structure of Polymer with Ethylene Glycol as a Solvent

3.2: Monomer Study

To rectify flexibility issues another monomer that cannot crosslink was introduced at the expense of the unsulphonated precursor. The dimethyldimethoxysilane (DMDMOS) was used to control the degree of crosslinking that was added at different percent compositions to observe changes in the film (Figure 3.9 for structure). Initially, this made brittle membranes that maintained their insolubility. However, with the increasing amount of DMDMOS the pieces exhibited greater relative flexibility. Also, the 20% DS was found to be soluble after observing previous solubility vials portraying that 20% DS was not stable in water over long periods of time. Based on these findings the DS was decreased to 10%. To determine why the membranes disintegrated into fragments with the addition of DMDMOS, TGA analysis was performed as shown in Figure 3.10. It was determined that the monomers were not fully reacting as evidenced by the monomer peaks in the 200-400˚C range, where only one was the sulphonate peak and the remainder

in this range was due to monomer. It was determined previously that sulphonate functional groups only produce one peak (Figure 3.3) when decomposing.

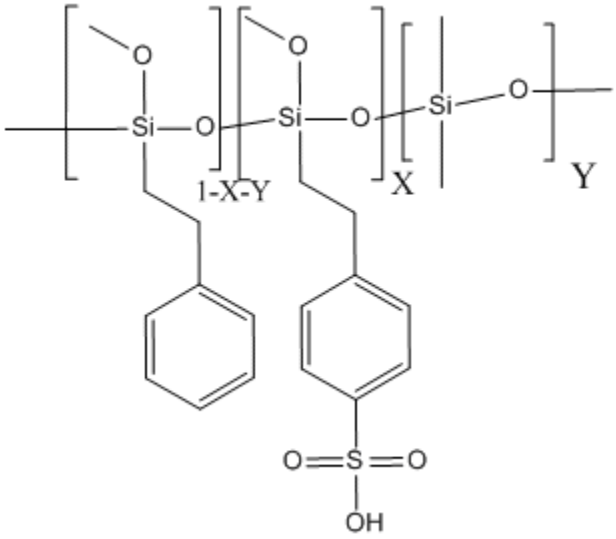

Figure 3. 9: Composition of a Copolymer synthesized from CSPETMOS, PETMOS and DMDMOS

3.3: Gellation

To promote the formation of higher quality membranes, the polymer solution was exposed to air (before casting) until the solution gelled in order to extend hydrolysis and condensation reactions. Further TGA analysis on the gelled membranes showed no unreacted monomer peaks as shown in Figure 3.11. Resultant membranes with fully reacted DMDMOS monomer were highly flexible and insoluble. These membranes swelled greatly in aqueous conditions becoming fragile after extended durations thus making them unsuitable for a fuel cell. Two membranes were synthesized with 10% DS with 30% and 10% DMDMOS. These membranes were ideal for a fuel cell, forming flexible membranes that were insoluble, and stable in water.

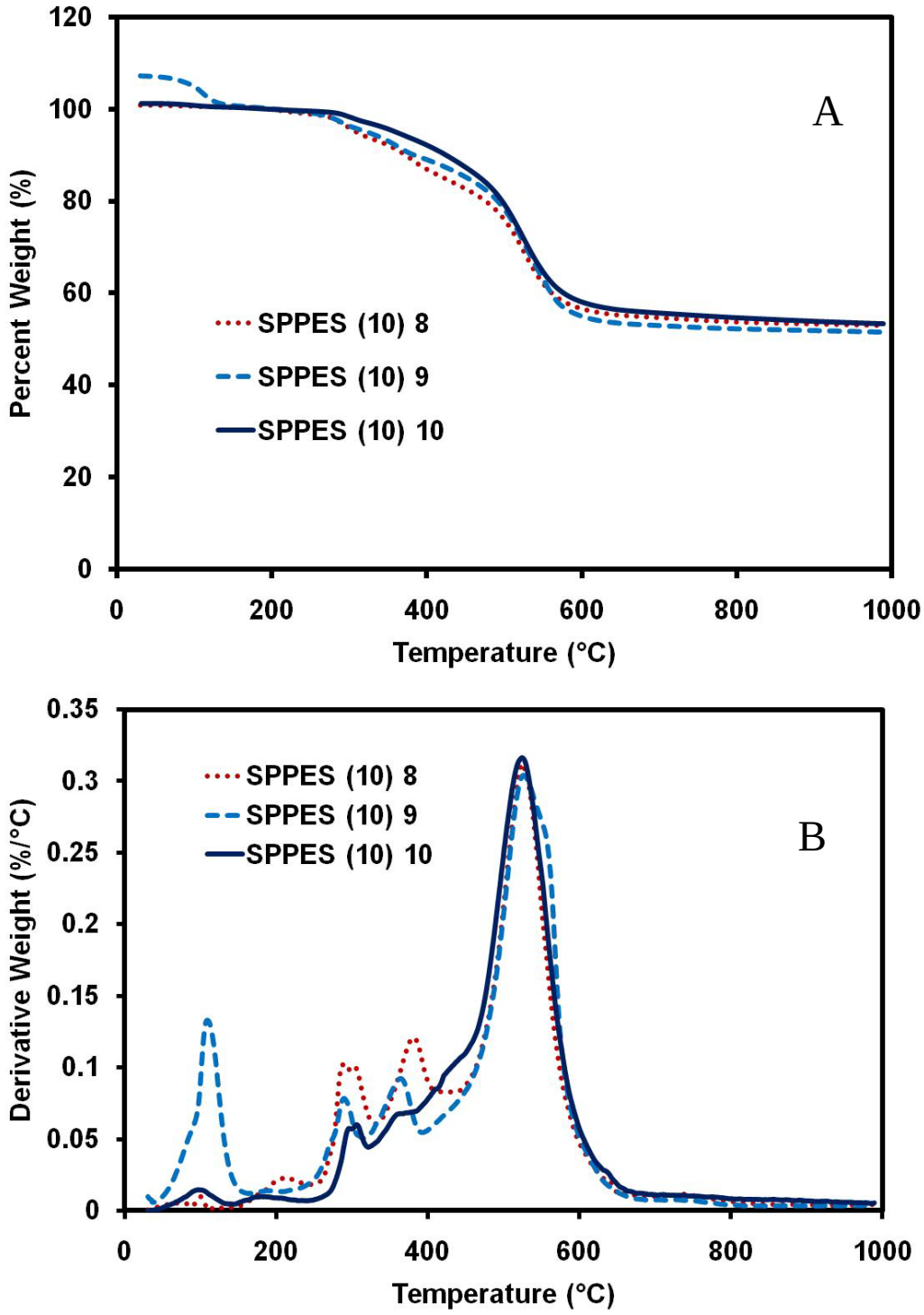

Figure 3. 10: Determination of Effects on Copolymer with Various amounts of DMDMOS to control level of crosslinking using SPPES (10) 8, SPPES (10) 9 and SPPES (10) 10 Decomposition Analysis A) Thermograph B) Derivative Thermograph

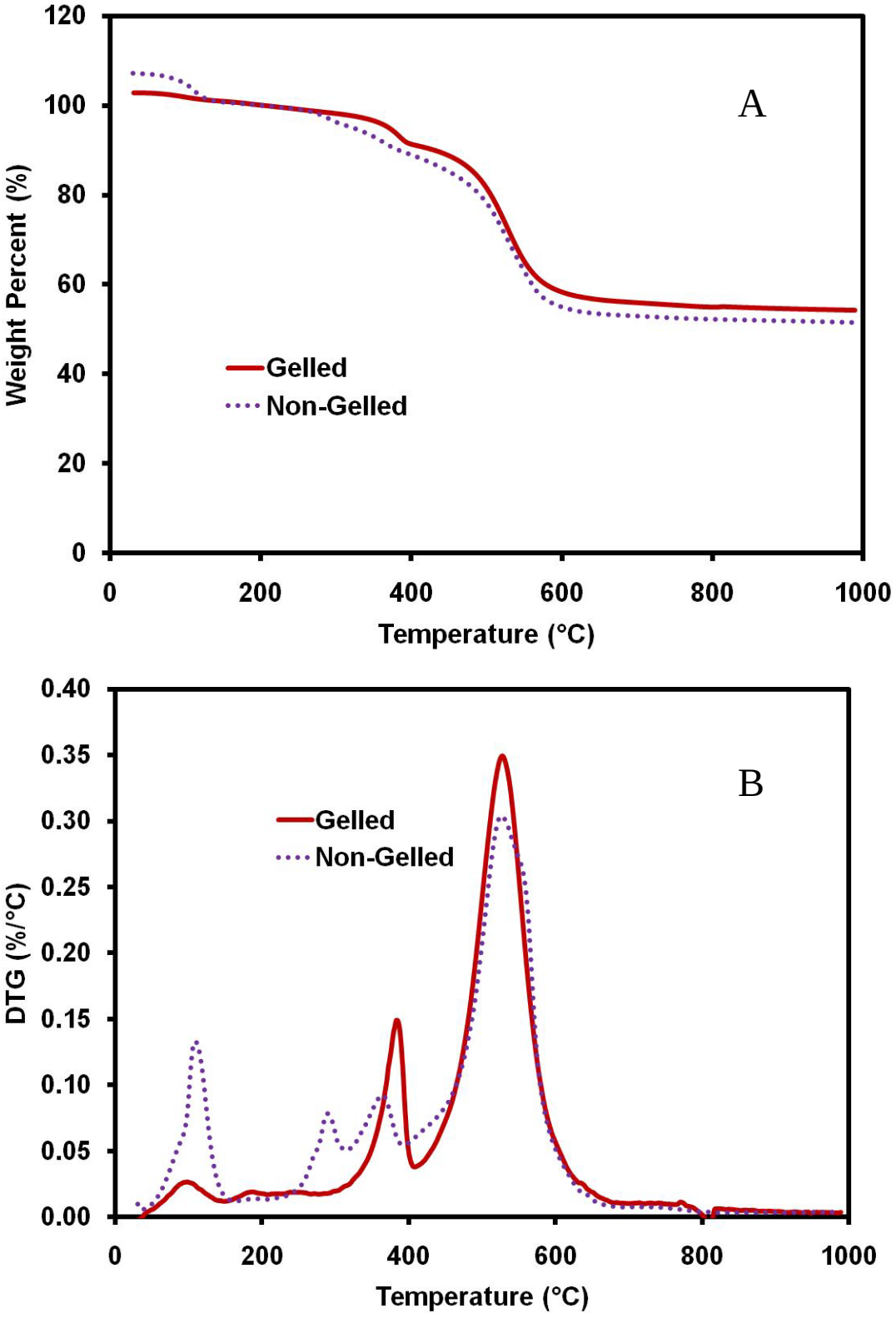

Figure 3. 11: Effect of Gellation before Casting using SPPES (10) 9 through Decomposition Analysis A) Thermograph B) Derivative Thermograph

3.4: Proton Conductivity

Insoluble and flexible membranes were placed in either an in-plane or through-plane conductivity cell. In-plane measurements are time efficient and simple. The x-intercept of this graph was the total resistance of the cell. The total resistance was due to the resistance of the cell (R_c) and the resistance of the membrane (R_m). To calibrate for R_c was to obtain the conductivity of Nafion with 1 layer then multiple layers to determine the R_c value. The determined R_c from the calibration was 0.0353Ω. With R_c known, the total resistance determined from the Nyquist plot was subtracted by the R_c value to obtain R_m. Conductivity was calculated with Equation 2.1 with the known R_m and thickness values. Since the resistance of the cell and membrane are both small and occur at the same point a greater error can occur.

For through-plane have a larger resistance due to the path for the current as seen in Figure 2.7. With semicircle Nyquist plots R_m was determined by fitting a semicircle, using Z plot, to the data to obtain the diameter. The diameter of the semicircle was the R_m, which is inserted into Equation 2.2 to determine the conductivity. Membranes SPPES (10) 9 and SPPES (10) 10 were initially tested in-plane cell, which resulted in Nyquit plots with no clear intercept due to high resistivity. When these samples were placed in a through-plane cell results indicated that the membranes were highly resistive and barely conductive from the resultant semicircles. Conductivity increases slightly as the amount of DMDMOS decreases as seen in Table 3.1. A SPPES (10) 11 was synthesized, however unlike its predecessors it dissolved in water. Due to the dissolution of the membrane at SPPES (10) 11 a membrane at SPPES (5) 12 was synthesized and its proton conductivity was measured. The membrane, while more conductive than samples

containing DMDMOS, was still less conductive than Nafion at 0.0420S/cm seen in Figure 3.12 and Table 3.1.

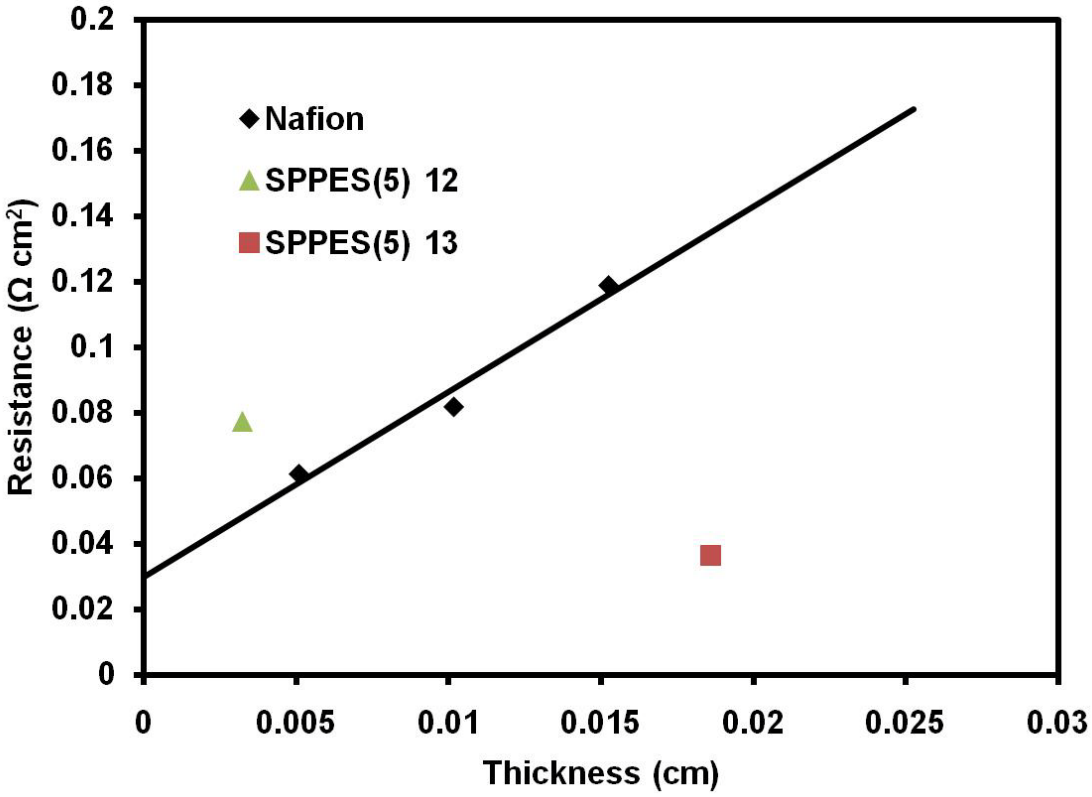

Figure 3. 12: SPPES(5) 12 and SPPES(5) 13 Comparison to Nafion 112 by In Plane Cell

3.5: Sulphonated Monomer Study

A sulphonated monomer without bulky functional groups was selected because of its inability to crosslink. The goal was to maintain flexibility and to target conductivity issues by using 3-(trihydroysilyl)-1-propanesulfonic acid (TPS) (Figure 3.13 for structure). Membranes produced were hydroscopic and highly flexible though unstable after extended periods of time under aqueous conditions. The SPPES (5) 13 was placed in an in-plane cell where the conductivity that this membrane exhibited was greater than Nafion being 0.513S/cm as seen in Figure 3.12 and Table 3.1. With such a high

conductivity and other beneficial properties this membrane has great potential to be placed in a fuel cell. However because of its hydroscopic nature the membrane absorbs large amounts of water and becomes fragile.

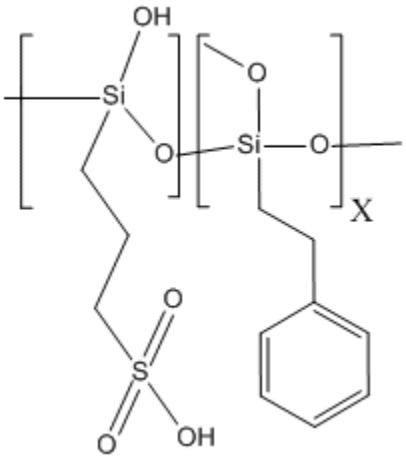

Figure 3. 13: Structure of Copolymer with TPS and PETMOS

3.6: Summary of Results

Conductivity measurements are seen in Figure 3.12 and summarized conductivity is depicted in Table 3.1. The SPPES (5) 13 is the most ideal membrane made for fuel cell applications. However due to its instability in water more research is needed to have this membrane be useful in fuel cell applications. This membrane was obtained by the optimization of a procedure to make an ideal PEM. Optimized parameters were a 6:1 water ratio, methanol as a solvent, 5% DS, gellation step and with a sulphonated with 3-(trihydrosilyl)-1-propanesulfonic acid.

3.7: Membrane Comparisons

Nafion is the most commonly accepted PEM, thus it is the standard to which all new materials are compared. Nafion has a proton conductivity of 0.0830 S/cm at standard conditions (25˚C, fully hydrated). In this chapter, two membranes were

synthesized that were able to fit the criteria to be suited for a fuel cell. Those membranes were the SPPES (5) 11 and SPPES (5) 13. For the SPPES (5) 11, the proton conductivity was determined to be 0.042 S/cm, which is approximately half that of Nafion. However, its conductivity is comparable to other alternative PEMs reported in the literature. For example, Easton et al. prepared S-PEEK membranes with various IECs which had conductivities ranging between 0.0052- 0.0381S/cm [37]. There are a plethora of hydrocarbon-based PEMs in the literature which have comparable conductivities [38]. There are relatively few reported of entirely polysiloxane-based PEMs in the literature. Gautier-Luneau et al. reported sulphonated polysiloxane membranes using benzyltriethoxysilane that were prepared with a similar method as was portrayed in this thesis [39]. One main difference was that the precursor Gautier-Luneau et al. used was not sulphonated therefore an additional step to sulphonate the polymer was necessary which was performed with chlorosulphonic acid. The membranes produced had a proton conductivity of 0.016 S/cm [39]. The proton conductivity determined for SPPES (5) 11 (0.513 S/cm) was significantly better than the Gautier-Luneau membranes.

Table 3. 1: Composition of Various Polymers and Copolymers and Properties

Code	CSPE-TMOS	PE-TMOS	DMDMOS	TPS	Soluble (Y/N)	Area Specific Resistance (Ωcm^2)	Proton Conductivity (S/cm)
SPPES(100)1	100	0	0	0	Y	N/A	N/A
SPPES(80)2	80	20	0	0	Y	N/A	N/A
SPPES(40)3	40	60	0	0	Y	N/A	N/A
SPPES(20)4	20	80	0	0	N →Y	N/A	N/A
SPPES(20)5	20	30	50	0	N	N/A	N/A
SPPES(20)6	20	50	30	0	N	N/A	N/A
SPPES(20)7	20	70	10	0	N	N/A	N/A
SPPES(10)8	10	40	50	0	N	N/A	N/A
SPPES(10)9	10	60	30	0	N	9.047	0.000742
SPPES(10)10	10	80	10	0	N	2.365	0.00184
SPPES(10)11	10	90	0	0	Y	N/A	N/A
SPPES(5)12	5	95	0	0	N	0.0772	0.0420
SPPES(5)13	0	95	0	5	N	0.03625	0.513
Nafion 112	N/A	N/A	N/A	N/A	N	0.0612	0.0830

Chapter 4

Composites

Results and Discussion

4.1: Composite Introduction

Sulphonated silanes are molecules that aid in proton conductivity and are hyrophillic. Combining sulphonated silane with Nafion producing a composite, is expected to have higher water retention and better proton conductivity. In this chapter 2-4-chlorosulphonylphenethyltrimethoxysilane (CSPETMOS) was used as the sulphontated monomer, which was used in the previous chapter as a proton conductor within the polymer structure. CSPETMOS was ideal due to its protected functional group, which deprotects in the presence of acid. When CSPETMOS was inserted into Nafion it does not react in side reactions due to its protection. Once in the pores of Nafion it deprotects from Nafion being in its acidic form. From the deprotection the sulphonate group is present to aid in proton conductivity. This reaction was more ideal due to the deprotection and insertion of the sulphonated precursor was one step compared to other two step methods (22). Optimization was undergone to determine the best conditions on controlling the SS loading within Nafion. This was done by investigating impregnation time, thickness of Nafion and concentration of the precursor. Nafion-CSPETMOS composite information are summarized in Table 4.1.

4.1.1: Impregnation Time

Composite membranes made with Nafion and silica material were synthesized using different parameters to obtain an ideal membrane. The first parameter looked at was impregnation time. An adapted procedure was used by Jung et al. who controlled the silica loading in Nafion by varying the impregnation time (18). Impregnation times of 9 (Nafion 112-CSPETMOS 1), 4.5 (Nafion 112-CSPETMOS 2), and 1 (Nafion 112-

CSPETMOSTMOS 3) min(s) were used to investigate the effect on loading while using our SS monomer. Silica loading was determined by combusting the composites with the TGA to determine the residual mass. After the full combustion study of the composite the material that did not decompose was the SiO_2. Since SiO_2 does not combust it can be determined the amount of SS was present in Nafion since it does not contain any silica originally. The SS loading was determined by the residual mass at (700˚C on TGA) divided by the dry mass (200˚C) as seen in the below sample calculation. As seen in Figure 4.1 the SS loading did not change within the composite membranes.

$$SS = \frac{Residual\ Mass}{Dry\ Mass} * 100\%$$

$$SS = \frac{0.1618mg}{1.4502mg} * 100\%$$

$$SS = 11.2\%$$

4.1.2: Thickness

To control SS loading, thicknesses of Nafion were investigated in order to control the loading more effectively since impregnation time did not affect the silica loading. Two thicknesses were compared to observe the loading by using Nafion 112 (Nafion 112-CSPETMOSTMOS 3) and 115 (Nafion 115-CSPETMOSTMOS 4). The residual mass leftover in the TGA from decomposing the samples were the same from the two thicknesses used. Therefore thickness does not play a role in the SS loadings based from the determined residual masses found in the TGA curve depicted in Figure 4.2.

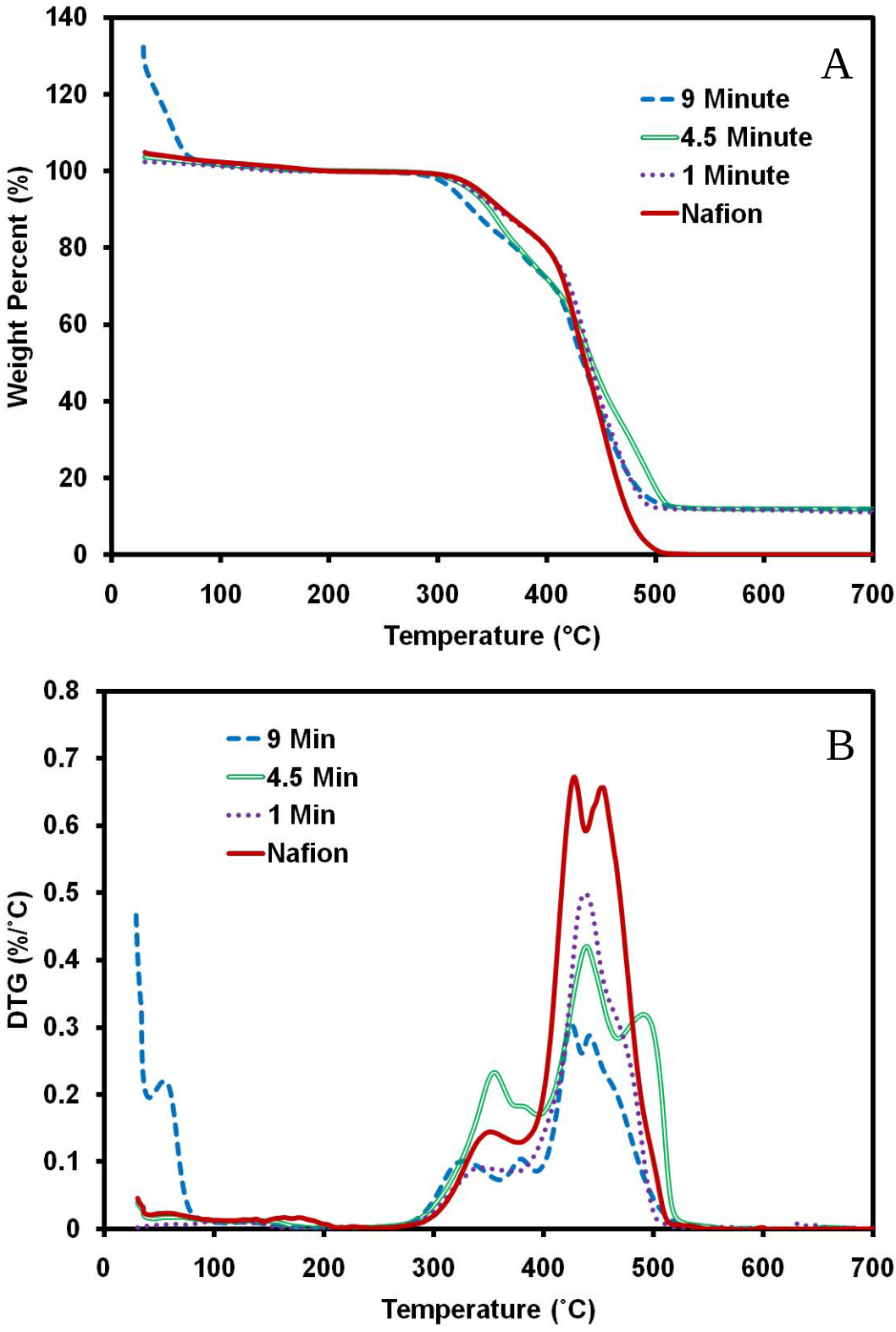

Figure 4. 1: Determination of SS Loading by varying Impregnation Time Combustion Analysis A) Thermograph B) Derivative Thermograph

4.1.3: Concentration

Due to impregnation time and thicknesses not affecting the silica loadings, the monomer concentration was changed. These concentrations were attained by changing the volume ratios of the required reactants (SS and MeOH). The methanol content was varied to minimize the SS concentration in the solution before introducing the solution to Nafion. Concentrations were performed by volume ratios that were 1:1 (Nafion 112-CSPETMOSTMOS 5) and 2:1 (Nafion 112-CSPETMOSTMOS 6) to control the silica loading. Decomposition of these composites showed differences in the residual masses from the TGA curves as seen in Figure 4.2A. By varying the reactant concentration ratios silica loadings were controlled. The SS loading decreased significantly from the 1:1 volume ratio of reactants to the 2:1 ratio based from the residual mass from the decomposition studies. As seen in Figure 4.2B in the 300-400˚C range depicts the sulphonate peak increasing accordingly to the addition of SS.

4.2: Characterization

4.2.2: Proton Conductivity Measurements under Various Humidities

Composites at different SS loadings were characterized to examine the effect on membrane properties. Samples were placed in a humidity chamber at 25˚C at various humidities to determine how composites performed in humidified and dry conditions. Figure 4.3 portrays the obtained Nyquist plot for the Nafion 112-CSPETMOS 3 composite with varied humidity. By determining the diameter of each semicircle, which was the resistance of the membrane, resistances over varied humidity can be obtained. Proton conductivity was determined at each RH.

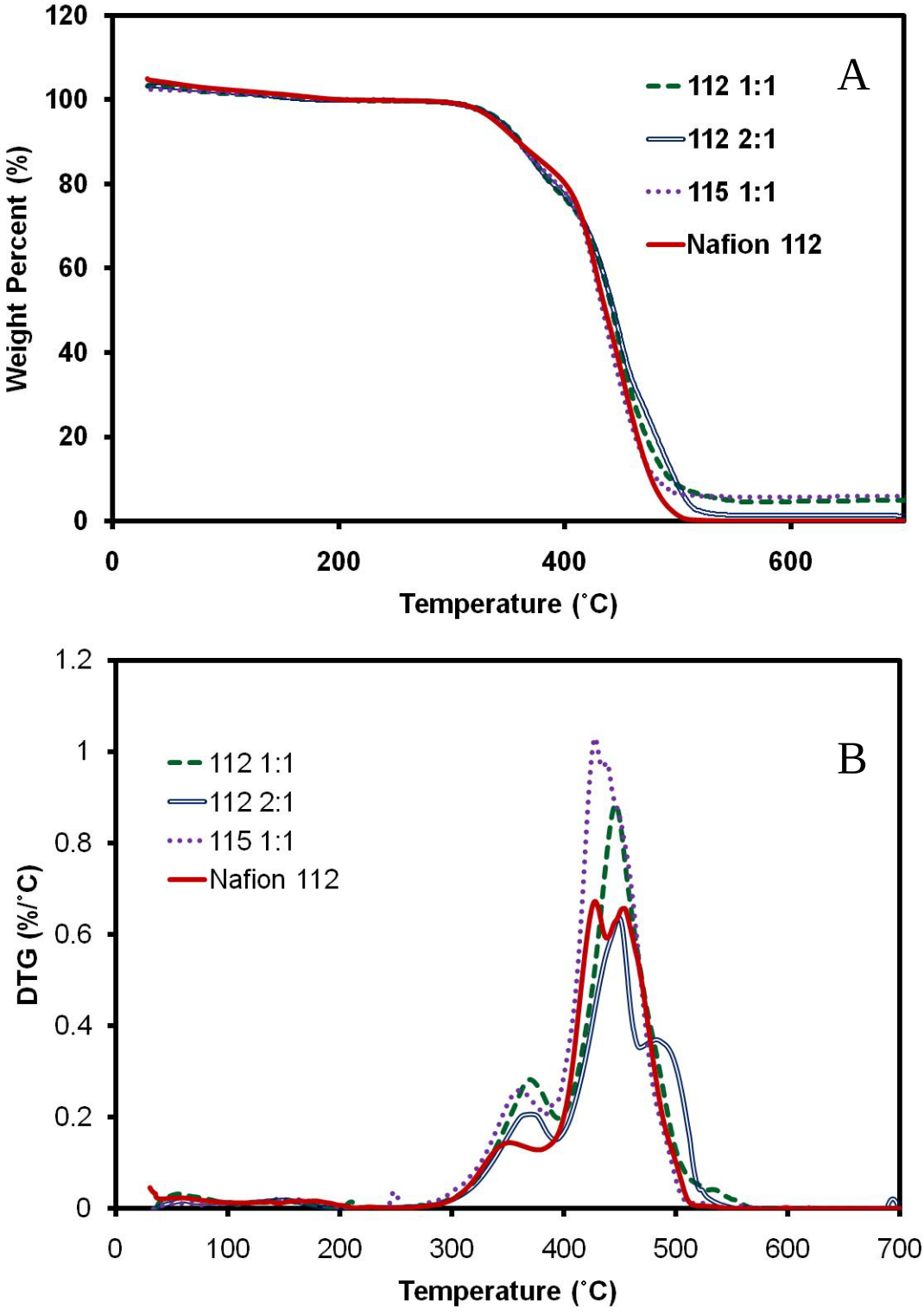

Figure 4. 2: Determination of SS Loading by varying Concentration and Thickness under Combustion Analysis A) Thermograph B) Derivative Thermograph

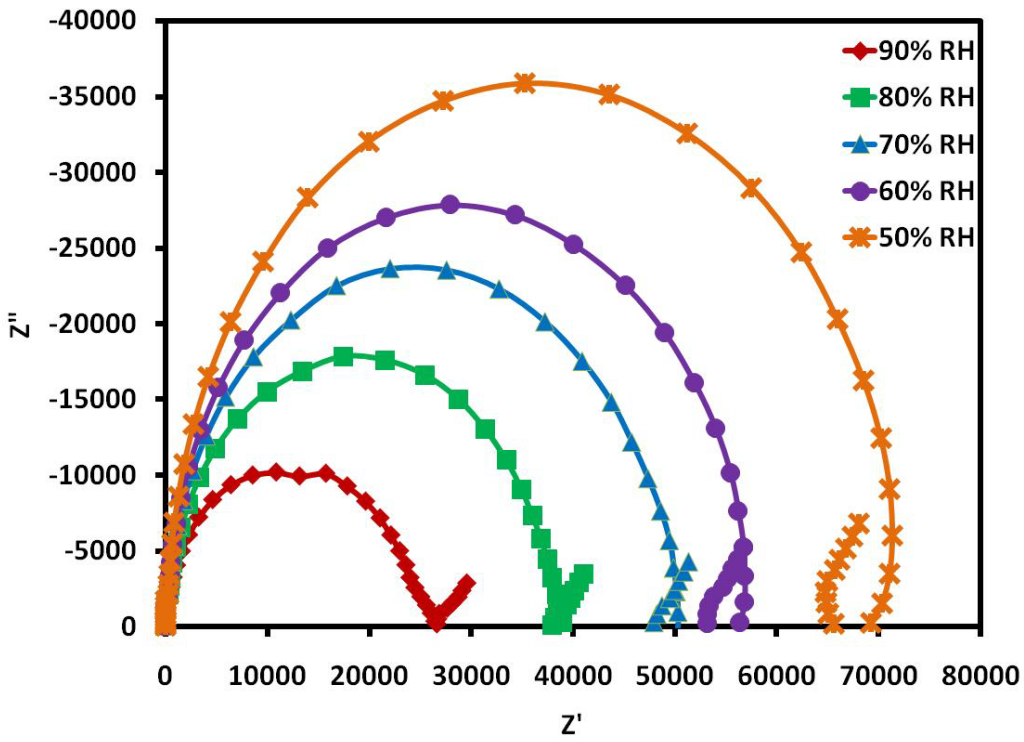

Figure 4. 3: EIS Determined Semicircles on Nyquit plot for Nafion 112-CSPETMOS 3

A plot of proton conductivity over varied humidity was performed on Nafion 112-CSPETMOS 6 and Nafion 112 as seen in Figure 4.4. At low SS loadings, 2.6% (Nafion 112-CSPETMOS 6), the observed proton conductivity was significantly better than Nafion. The conductivity obtained at low humidity (50%RH) was higher than Nafion in its peak conditions (90%RH) showing that low SS loadings can improve conductivity in dry environments. Figure 4.4 demonstrates that when SS loadings are high, 11.2% (Nafion 112-CSPETMOS 3); the composite behaves similar to Nafion however has higher conductivity in humidified environments due to retaining more water. This was due to the SS material inserted into Nafion was blocking the protons from travelling

through the membrane. This showed how important it was to balance SS content in Nafion to be able to conduct protons and not block pores.

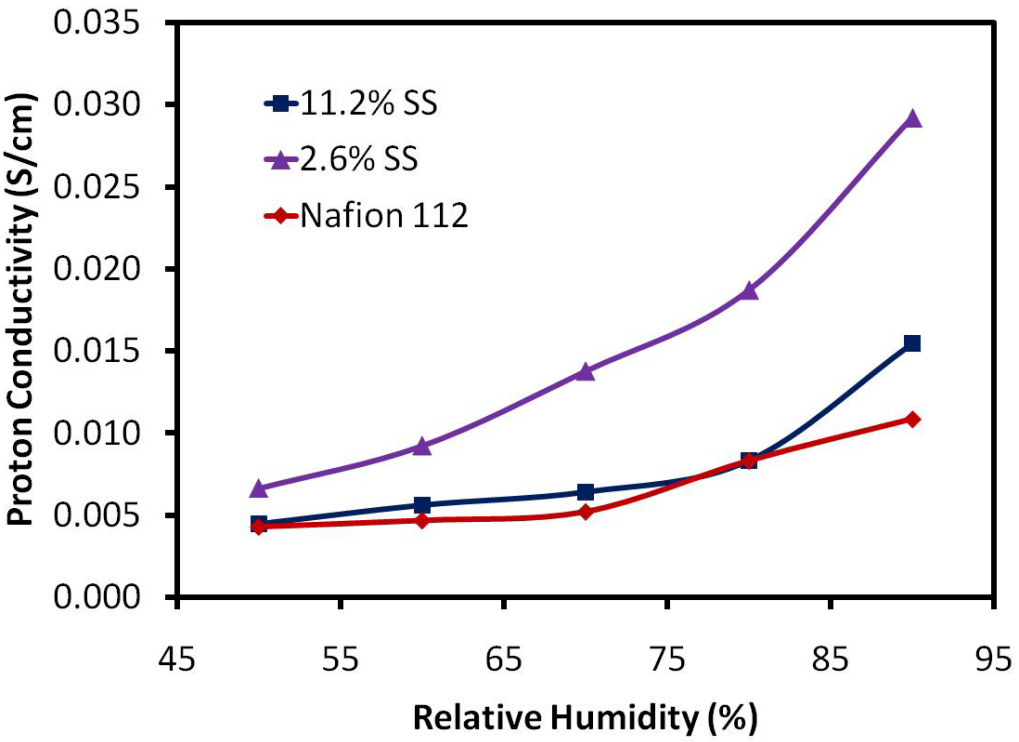

Figure 4. 4: Proton Conductivity at Various Humidities at Constant 25˚C

Table 4.1: Summary of Proton Conductivities at Various Humidities

Sample	SS Loading	Humidity (%RH)	Conductivity (S/cm)
Nafion 112	N/A	90	0.010844
		50	0.004305
Nafion 112-CSPETMOS 3	11.2%	90	0.015449
		50	0.004467
Nafion 112-CSPETMOS 6	2.6%	90	0.029208
		50	0.006646

4.2.2: Proton Conductivity Measurements under varied Temperature

Measurements for proton conductivity while varying temperature was conducted by the same method as seen above in section 4.3.1 except that temperature was varied

and humidity kept constant at 95%RH. Low SS composites displayed better conductivities than the high SS composite and Nafion as seen in Figure 4.5. Both Nafion and Nafion 112-CSPETMOS 5 displayed increasing proton conductivity with temperature. However, the conductivity of Nafion 112-CSPETMOS 3 levelled-off at temperature above 60˚C. Overall, Nafion 112-CSPETMOS 5 displayed the highest conductivity at all temperature. In Figure 4.5 Nafion and Nafion 112-CSPETMOS 3 have a nonlinear relationship between conductivity and temperature, where Nafion 112-CSPETMOS 5 has a more linear relationship. In an Arrhenius plot for Nafion and Nafion 112-CSPETMOS 3 depicts a typical linear relationship as seen in Figure 4.6. For Nafion and Nafion 112-CSPETMOS 5 (11.2% SS) have reasonable fitting of the data allowed for to determination the activation energy for proton conductivition. Values of 19.78 and 15.04 kJ/mol were determined for Nafion and Nafion 112-CSPETMOS 5 (11.2% SS), respectively. However, Nafion 112-CSPETMOS 3 produced a nonlinear Arrhenius plot would have a poor linear fit, as seen in Figure 4.7. This indicates that there were two activation energies which occur at low and high temperatures. Estimated activation energies for Nafion 112-CSPETMOS for low and high temperatures were 12.17 and 3.36 kJ/mol, respectively. These values are considered estimates since four data points are insufficient for rigorous fitting at both high and low temperature. Additional data would need to be obtained to determine accurately the activation energies at both low and high temperature. Nonetheless, the estimated values provide valuable information about this membrane.

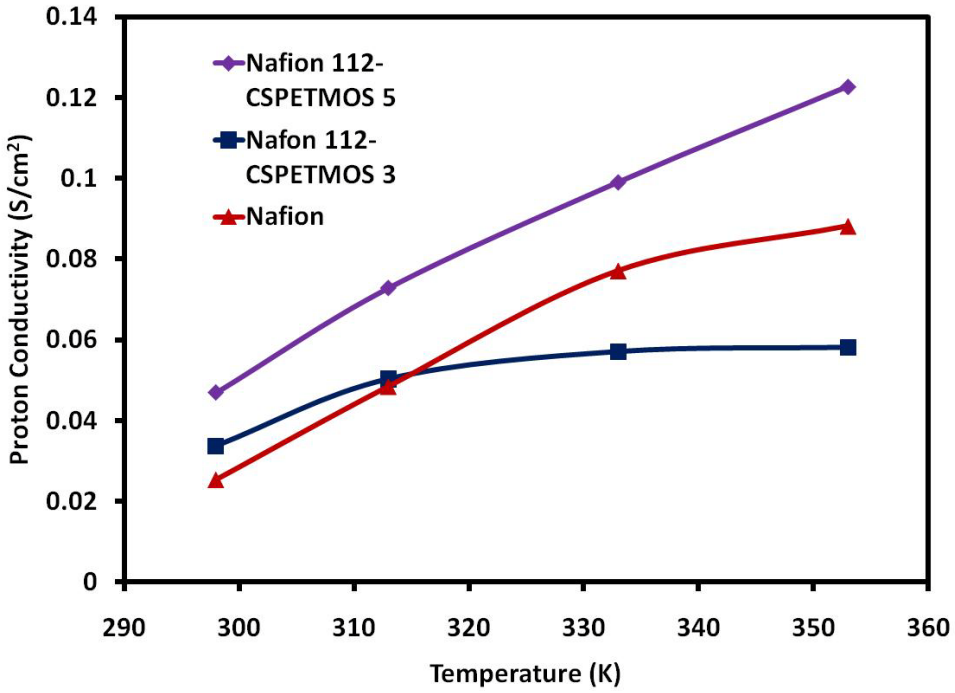

Figure 4. 5: Proton Conductivity at Various Temperatures at Constant 95%RH

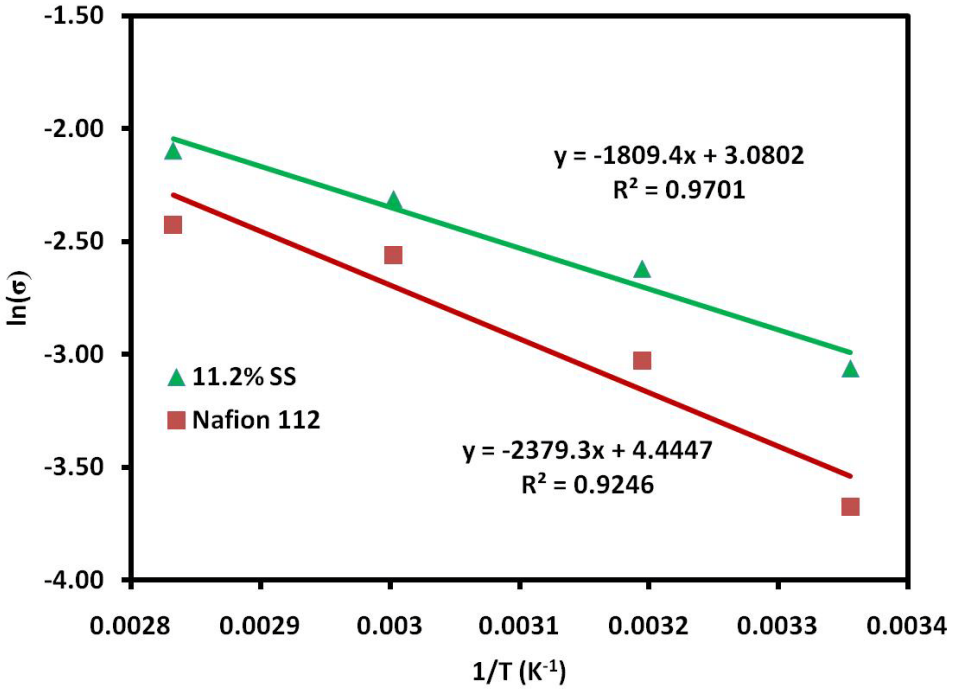

Figure 4. 6: Energy Activation Determination of A) Nafion 112 B) Nafion 112-CSPETMOS 3

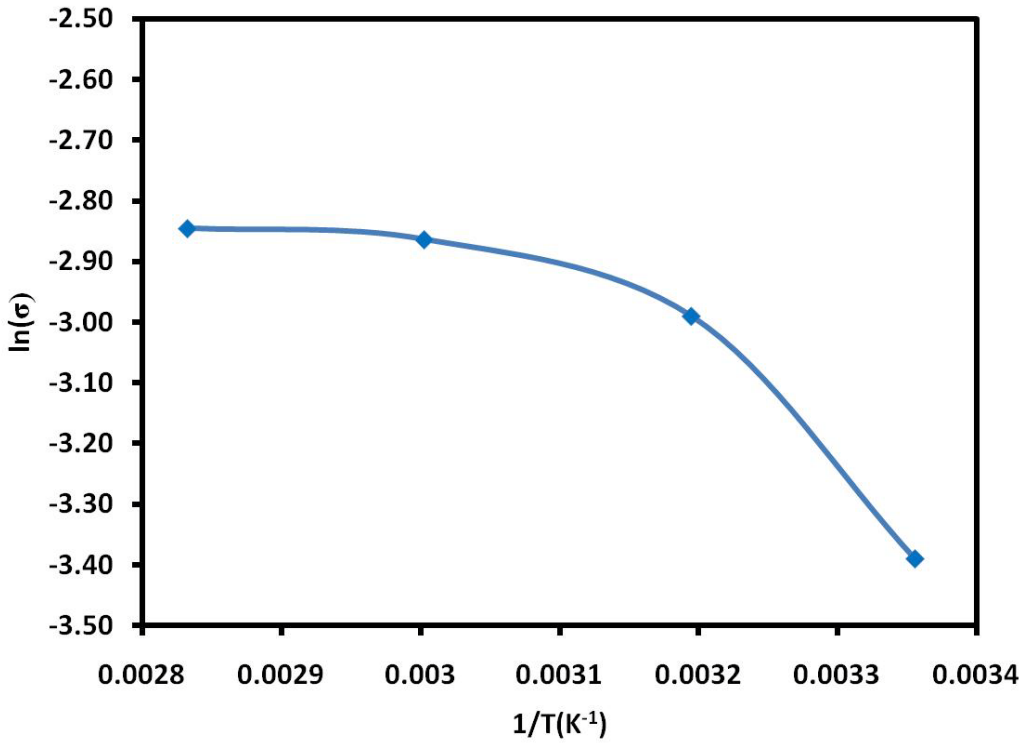

Figure 4.7: Arrhenius Plot for Nafion 112-CSPEPETMOS 5

4.2.3: Fuel Cell Performance

The composites membranes were placed into a fuel cell to observe how the SS loadings affect fuel cell performance. Ideal polarization curves would produce the most power based from the obtained potentials and voltage. For example, Equation 4.1 shows that the higher of both current (I) and potential (V) is the more power that is produced.

$$Power = I * V \qquad \textbf{Equation 4.1}$$

Figure 4.8 depicts performance data obtained by 2.6% SS (Nafion 112-CSPETMOS 6), Nafion and Nafion 115-CSPETMOS 4, which has a 5.9% SS. The performance data was taken with humidified gas feeds which were at 100% RH at 30˚C, where Nafion and Nafion 115-CSPETMOS 4 had similar trends throughout the polarization curve.

However, Nafion 112-CSPETMOS 6 had significantly higher performance and this was due to the SS increasing its proton conductivity. During operation at 50˚C, 60%RH Nafion 115-CSPETMOS 4 had considerable flooding, which resulted in no performance being able to be recorded therefore being omitted from future graphs seen in Figure 4.9A. With high water content within the MEA as well as pores being blocked by the SS performance dropped significantly. However with higher temperatures (70˚C and 64%RH) Nafion 112-CSPETMOS 6 had the better performance at higher current compared to Nafion (which dried out), which can be seen in Figure 4.9B. It was unclear that at lower current Nafion had better performance than Nafion 112-CSPETMOS 6. Overall, Nafion 112-CSPETMOS 6 had the best performance by the ability to maintain the high current in dry conditions from better water retention.

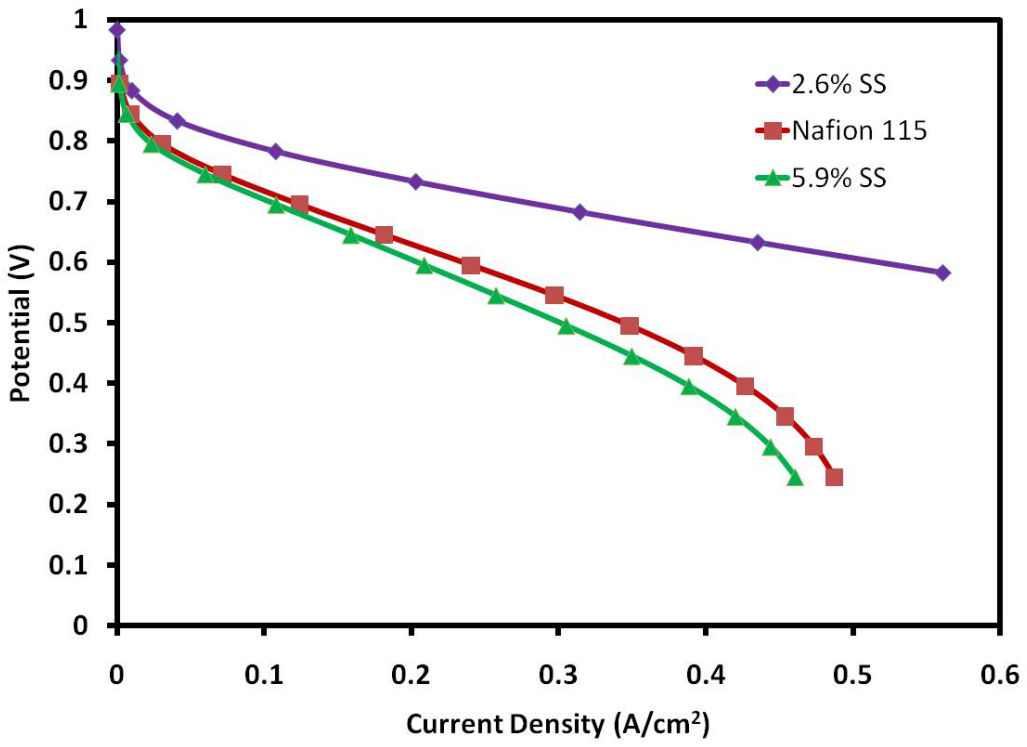

Figure 4. 8: Fuel Cell Polarization Curves at 30˚C and 100%RH

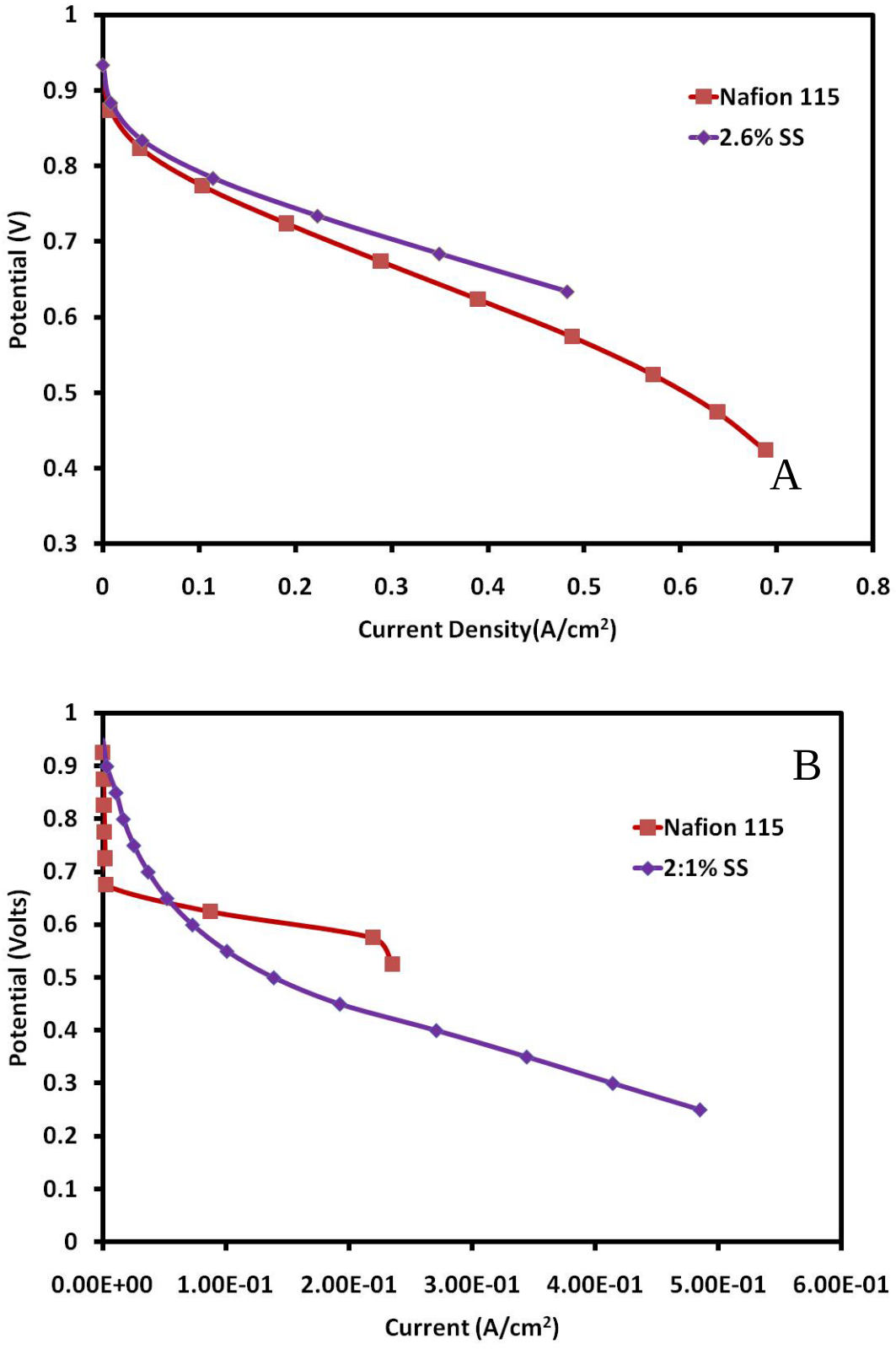

Figure 4. 9: Performance Curves for Nafion 112-CSPETMOS 6 A) 50˚C 60%RH B) 70˚C 64%RH

4.3: Summary

Impregnation time does not play a role in controlling the silica loading. However, varying the concentration of the silica solution controls the silica loading in the composites at a greater efficiency. High silica loadings resulted in blocked pores within Nafion causing higher resistance and lower performance both in proton conductivity and fuel cell testing. Lower silica loading composites have considerable higher performance in dry conditions at both low and high temperatures indicating a low silica loading was ideal to maintain water within the membrane without blocking pores.

4.4: Membrane Comparison

At standard conditions (25˚C, fully hydrated) Nafion displayed higher proton conductivity than composites produced here. However, regarding performances at dry conditions and high temperature low sulphonated silica loading surpassed Nafion's capabilities by retaining water content and improving proton conductivity. Jung el al. synthesized composites using TEOS as a precursor obtained proton conductivity at standard conditions to be the same as Nafion being approximately 0.08 S/cm [19]. Ren et al. synthesized composites using thiol based precursor with a post sulphonation step [22]. It was determined that their proton conductivity was 0.0091S/cm at standard conditions and all of their fuel cell performance performed worse than Nafion [22]. The composites synthesized for this thesis had better performance than Nafion and better proton conductivities under dry conditions. Therefore, these membranes are promising candidates to for use under high temperature/low RH conditions.

Activation energy depicts the energy required to conduct protons across the membrane. Lavorgna et al. reports the activation energy for Nafion to be 19.4 kJ/mol for Nafion, which was similar to the value obtained in this thesis of 19.8kJ/mol (39). Nafion 112-CSPETMOS 3 was 15.0kJ/mol. For comparison, Lavorgna et al reported an Ea value of 15.2kJ/mol for a Nafion/SiO_2 membrane that was made from TEOS precursor (39). The low sulphonated silane composite Nafion 112-CSPETMOS 5 that has two activation energies are estimated to be 12.17 and 3.36 kJ/mol respectively portraying promising characteristics of achieving expanding Nafion's capabilities at high temperature and dry conditions. Ren et al. obtained performance data for their thiol based composites, where their performances were worse than Nafion [22]. Composites depicted in this thesis have performances better than Nafion in most cases. Ren's composites have an extra step in their synthesis because of the post sulphonation that is required to obtain the sulphonate functional groups. The composites presented here have better properties and have fewer steps in the synthesis. Lower sulphonated silica loadings are better because there is a larger free volume within the pores of Nafion to accommodate water. While sulfonated silica is highly hydrophilic, it does occupy volume within the pore. Thus, there is a limit to the amount of water that can be accommodated within the pores. At high sulphonated silica loadings, this pore volume available to retain water is relatively low. Low to moderate loading of sulphonated silica appear to be optimal in that they not only have the ability to enhance proton conduction, but also have sufficient pore volume to accommodate a significant amount of water to aid in its conduction.

Table 4.2: Composition of Various Composites

Code	Impregnation Time	Volume Ratio of SS:MeOH	SS Loading	Resistance	Proton Conductivity
Nafion 112	N/A	N/A	N/A	0.0612	0.0830
Nafion 112-CSPETMOS 1	9	1:1	11.9	N/A	N/A
Nafion 112-CSPETMOS 2	4.5	1:1	11.8	N/A	N/A
Nafion 112-CSPETMOS 3	1	1:1	11.2	5814.6	0.0337
Nafion 115-CSPETMOS 4	1	1:1	5.9	0.26336	0.0577
Nafion 112-CSPETMOS 5	1	1:1	5.0	0.08952	0.0704
Nafion 112-CSPETMOS 6	1	2:1	2.6	0.08234	0.0765

Chapter 5

Conclusions and Future Directions

5.1 Conclusion

Optimization was performed on a procedure to produce polysiloxane membranes to be used for a hydrogen fuel cell. The conditions were using a 6:1 water to ensure appropriate amount of hydrolysis to have all the monomers react. Concentration was determined to be 0.49M which gave polymers with reasonably high molecular weight. DS was determined to be approximately 5% to prevent solubility and minimize swelling in water while maintaining proton conductivity. Reaction temperature was established to be 60˚C, the highest temperature methanol can be used for reflux to ensure completion of hydrolysis and condensation reactions. A crosslinking investigation was conducted to observe if this would solve flexibility issues. DMDMOS provided some flexibility however made the membranes highly resistive with limited conductivity. However, with the addition of a gellation step (rather than casting straight into a dish) produced membranes that were highly flexible. Membranes made with 0% DMDMOS and were gelled with a 5%DS had low conductivity. An alternate sulphonated monomer was studied with a less bulky functional group. These membranes were highly conductive. With the optimization efforts the membranes made for purely polysiloxanes were unstable in water for fuel cell purposes.

Composite membranes were another method to target higher temperature and low RH application by inserting SS into the pores of Nafion. Impregnation time to insert SS had no effect in varying the silica loading into the membranes. Changing the sulphonated silane concentration was able to control the loadings into the pores. Nafion/SS composite membranes retained more water and maintained its conductivity under dry conditions. Under dry conditions and high temperature the composite with low SS exhibited

conductivities on par with Nafion in wet conditions. High SS blocked the pores and water was not able to maintain in the pores and perform just as Nafion did itself. With varied temperature high SS had steady performance throughout producing higher proton conductivities. Fuel cell testing showed that 2.6% SS composite produced more power overall than Nafion, where the higher loadings of SS flooded during use. In conclusion, to improve Nafion's properties at high temperature and/ or low humidity, low sulphonated silane loadings were optimal.

5.2 Future Directions

One future study would to be to improve polysiloxane membranes to be more stable in water. A possible solution would be performing triple layers on the membranes to be able to coat them so water would not penetrate the membranes (41). As seen in Figure 5.1 depicts how the layers in a triple layer would be positioned.

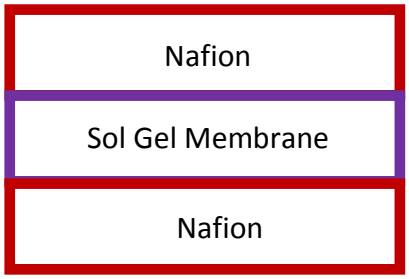

Figure 5. 1: Orientation of Constituents for a Triple Layer involving Nafion and Sol Gel Membrane

The thickness that a TPS membrane contained while having high proton conductivity makes it more suited for another application. Therefore, an investigation would include using sulphonated polysiloxane membranes sulphonated by TPS for use in sensors due to its high proton conductivity. For a membrane to be used for sensors it

must have a good pore structure in order for the chemical or gas to pass through the membrane in a controlled manner (42). An investigation would be required on the membrane's pore structure for a sensor application.

Due to the polysiloxane being produced by a self assembly method another investigation could be to compare these membranes to template assisted produced membranes of the same material (31). This investigation would provide insight to how membrane structure affects membrane properties.

Potential uses for composite membranes would be in a copper chloride process that requires a membrane that copper cannot permeate through. The copper chloride process is a method in producing hydrogen in a cheap and energy efficient way (42). The main problem of using this cycle is copper crossover (43). Therefore, using membranes where their pores are blocked would be ideal to eliminate copper crossover. Samples have been sent to industry for testing in this area.

Another use for composite membranes would be for direct methanol fuel cells. One of the issues with this fuel cell is methanol crossover, which causes a loss in energy (44). Therefore, using composites with highly blocked pores would be ideal for this application as well. An investigation would be needed to observe the amount of methanol crossover that would be produced.

Chapter 6

References

1) Ormerod, R. (2003) Chemical Society Reviews: Solid Oxide Fuel Cells. 32: 17-28.

2) Wasmus, S., and Kuver, A. (1999) Journal of Electroanalytical Chemistry: Methanol Oxidation and Direct Methanol Fuel Cells: A Selective Review. 461: 14-31.

3) Barbir, F., and Gomez, T. (1996) International Journal of Hydrogen Energy: Efficiency and Economics of Proton Exchange Membrane (PEM) Fuel Cells. 21: 891-901.

4) Carrette, L., Friedrich, K.A., Stimming, U. (2000) Fuel Cells: Principles, Types, Fuels and Applications. Chemphyschem. 1: 162-193.

5) O'Hayre, R., Cha, S., Colella, W., and Prinz, F. (2009) Fuel Cell Fundamentals. 2nd ed. Wiley: USA. Pg 263-266.

6) EG&G Technical Services. (2004) Fuel Cell Handbook. 7th ed. U.S Department of Energy: West Virginia. Pg 3-1 – 3-6.

7) Eastcott, J., and Easton, E.B. (2009) Electrochimica Acta: Electrochemical Studies of Ceramic Carbon Electrodes for Fuel Cell Systems: A Catalyst Layer without Sulfonic Acid groups. 54: 3460-3466.

8) Cheng, X., Shi, Z., Glass, N., Zhang, L., Zhang, J., Song, D., Liu, Z., Wang, H., and Shen, (2007) J. Journal of Power Sources: A review of PEM hydrogen fuel cell contamination: Impacts, mechanisms, and mitigation. 165: 739-756.

9) Larminie, J., and Dicks, A. (2003) Fuel Cell Systems Explained. 2nd ed. Wiley: England. Pg 67-71.

10) Kreuer, K.O. (1996) Chemistry of Materials: Proton Conductivity: Materials and Applications. 8: 610-641.

11) Majsztrik, P., Bocarsly, A., and Benziger, J. (2008) Journal of Physical Chemistry B: Water Permeation through Nafion Membranes: The Role of Water Activity. 112: 16280-16289.

12) Riascos, L., Pereira, D. (2009) Journal of the Electrochemical Society: Limit Operating Temperature in Polymer Electrolyte Membrane Fuel Cells. 156: B1051-B1058.

13) Zhang, J., Tang, Y., Song, C., Cheng, X., Zhang, J., Wang, H. (2007) Electrochimica Acta: PEM Fuel Cells operated at 0% Relative Humidity in the Temperature Range of 23-120˚C. 52: 5095-5101.

14) Xu, H., Song, Y., Russell Kunz, H., and Fenton, J. (2005) Journal of the Electrochemical Society: Effect of Elevated Temperature and Reduced Relative Humidity on ORR Kinetics for PEM Fuel Cells. 152: A1828-A1836.

15) Bai, H., and Ho, W. (2008) New poly(ethylene oxide) soft segment-containing sulfonated polyimide copolymers for high temperature proton-exchange membrane fuel cells. Journal of Membrane Science. 313: 75-85.

16) Lufrano, F., Squadrito, G., Patti, A., Passalacqua, E. (1999) Journal of Applied Polymer Science: Sulfonated Polysulfone as Promising Membrane for Polymer Electrolyte Fuel Cells. 77: 1250-1257.

17) Mauritz, K., and Moore, R. (2004) State of Understanding of Nafion. Chemical Reviews. 104: 4535-4585.

18) Colomer, M., and Anderson, M. (2001) Journal of Non-Crystalline Solids: High Porosity Silica Xerogels Prepared by a Particulate Sol-gel Route: Pore Structure and Proton Conductivity. 290: 93-104.

19) Jung, D., Cho, S., Peck, D., Shin, D., Kim, J. (2002) Journal of Power Sources: Performance Evaluation of a Nafion/silicon Oxide Hybrid Membrane for Direct Methanol Fuel Cell. 106: 173-177.

20) Miyake, N., Wainright, J., and Savinell, R. (2001) Journal of the Electrochemical Society: Evluation of Sol-Gel Derived Nafion/Silica Hybrid Membrane for Proton Electrolyte Membrane Fuel Cell Applications I. Proton Conductivity and Water Content. 148-A898-A904.

21) Ye, G., Hayden, C., and Goward, G. (2007) Macromolecules: Proton Dynamics of Nafion and Nafion/SiO Composites by Solid State NMR and Pulsee Field Gradient NMR. 40: 1529-1537.

22) Ren, S., Sun, G., Li, C., Liang, Z., Wu, Z., Jin, W., Qin, X., and Yang, X. (2006) Journal of Membrane Science: Organic Silica/Nafion Composite Membrane for Direct Methanol Fuel Cells. 282: 450-455.

23) Sambandam, S., and Ramani, V. (2007) Journal of Power Sources: SPEEK/ Functionalized Silica Composite Membranes for Polymer Electrolyte Fuel Cells. 170: 259-267.

24) Pierre, A., and Pajonk, G. (2002) Chemistry of Aerogels and Their Applications. Chemical Reviews. 102: 4243-4266.

25) Jeong, M., Lee, K., Hong, Y., and Lee, J. (2008) Journal of Membrane Science: Selective and Quantitative Sulfonation of Poly(arylene ether ketone)s containing Pendant Phenyl Rings by Chlorosulfonic Acid. 314: 212-220.

26) Mauritz group. <http://www.psrc.usm.edu/mauritz/solgel.html> accessed February 15, 2009.

27) Brinker, C. (1988) Hydrolysis and Condensation of Silicates: Effects on Structure. Journal of Non-Crystalline Solids. 100: 31-50

28) Mukkamala, R., and Cheung, H. (1997) Journal of Materials Science: Acid and Base Effects on the Morphology of Composites from Microemulsion Polymerization and Sol-Gel Processing. 32: 4687-4692.

29) Brinker, J. (2006) Collodial Silica: Fundamentals and Applications. Taylor and Francis Group. Pg 615-635.

30) Allcock, H. (2008) Introduction to Materials Chemistry. Wiley: New Jersey, USA. Pg. 118- 154.

31) Lu, Z., Namboodiri, A., and Collinson, M. (2008) Self-Supporting Nanopore Membranes with Controlled Pore Size and Shape. Journal of the American Chemical Society. 2: 993-999.

32) Loveday, D., Peterson, P., and Rodgers, B. (2004) JCT Coatings Tech: Evaluation of Organic Coatings with Electrochemical Impedance Spectroscopy Part 1: Fundamentals of EIS. Analytical series: 46-52.

33) Easton, E.B. (2003) Chemical Modification of Fuel Cell Catalysts and Electrochemistry of Proton Exchange Membrane Fuel Cell Electrodes. National Library of Canada: 159-162.

34) Soboleva, T., Xie, Z., Shi, Z., Tsang, E., Navessin, T., and Holdcroft, S. (2008) Investigation of the through plane impedance technique for evaluation of anisotropy of proton conducting polymer membranes. Journal of Electroanalytical Chemistry. 622: 145-152.

35) Lin, H., Zhao, C., Ma, W., Shao, K., Li, H., Zhang, Y., and Na, H. (2010) Journal of Power Sources: Novel Hybrid Polymer Electrolyte Membranes Prepared by Silane-cross-linking Technique for Direct Methanol Fuel Cells. 195: 762-768.

36) Yang, S., Jang, W., Lee, C., Shul, Y., and Han, H. (2005) Journal of Polymer Science: The Effect of Crosslinked Networks with Poly(Ethylene Glycol) on Sulfonated Polyimide for Polymer Electrolyte Membrane Fuel Cell. 43: 1455-1464.

37) Easton, E.B., Astill, T., and Holdcroft, S. (2005) Journal of the Electrochemical Society: Properties of Gas Diffusion Electrodes Containing Sulfonated Poly(ether ether ketone). 152: A752- A758.

38) Smitha, B., Sridhar, S., and Khan, A. (2005) Journal of Membrane Science: Solid Polymer electrolyte membranes for fuel cell applications- a review. 259: 10-26.

39) Gautier-Luneau, I., Denoyelle, A., Sanchez, Y., and Poinsignon, C. (1992) Organic-Inorganic Photonic Polymer Electrolytes as Membranes for Low-Temperature Fuel Cell. Electochimica Acta. 37: 1615-1618.

40) Lavorgna, M., Gilbert, M., Mascia, L., Mensitieri, G., Scherillo, G., and Ercolano, G. (2009) Journal of Membrane Science: Hybridization of Nafion

membrane with an acid functionalised polysiloxane: Effect of morphology on water sorption and proton conductivity. 330: 214-226.

41) Martino, F. D., Vatistas, N. & Tricoli, V. (2009) Journal of the Electrochemical Society: Concept to Design for PEMFC: Triple-Layer Ion-Conducting Membrane. 156: B59-B65.

42) Estella, J. Echeverria, J.C., Laquna, M., and Garrido, J. (2007) Journal of Non-crystalline Solids: Silica xerogels of tailored porosity as support matrix for optical chemical sensors. Simultaneous effect of pH, ethanol:TEOS and water:TEOS molar ratios, and synthesis temperature on gelation time, and textural and structural properties. 353: 286-294.

43) Santhanam, R, and Easton, E.B. (2010) International Journal of Hydrogen Energy: High performance ceramic carbon electrode-based anodes for use in the Cu-Cl thermochemical cycle for hydrogen production. 35: 1001-1007.

44) Easton, E.B., Langsdorf, B. Hughes, J. Sultan, J., Qi, Z., Kaugman, A., and Pickup, P. (2003) Journal of the Electrochemical Society: Characteristics of Polypyrrole/Nafion Composite Membranes in a Direct Methanol Fuel Cell. 150: C735-C739.

Chapter 7

Appendix

Figure 1.1

Sure, no problem. You can use this e-mail as your authorization request.

Best Regards,

Javier Castano
University Press of the Pacific

At 19:00 11/03/2010, you wrote:

March 11, 2010

Fuel Cell Handbook 7th Edition

I am preparing my master?s of science thesis for submission to the Office of Graduate Studies at the University of Ontario Institute of Technology (UOIT) in Oshawa, Ontario, Canada. I am seeking your permission to include a figure from the above publication described below.

Fuel Cell Handbook 7th Edition from EG&G Technology Services, INC, page 3-2 Figure 3-1a from 2005 ISBN: 1410219607

Canadian graduate theses are reproduced by the Library and Archives of Canada (formerly National Library of Canada) through a non-exclusive, world-wide license to reproduce. Loan. Distribute. Or sell theses. I am also seeking your permission for the material described above to be reproduced and distributed by the LAC(NIL). Further details about the LAC(NLC) thesis program are available on the LAC(NLC) website (www.nlc-bnc.ca).

Full publication details and a copy of this permission letter will be included in the thesis.

Yours sincerely,

Nicole De Almeida
Master?s Candidate

Figure 1.8

This is a License Agreement between Nicole E De Almeida ("You") and American Chemical Society ("American Chemical Society") provided by Copyright Clearance Center ("CCC"). The license consists of your order details, the terms and conditions provided by American Chemical Society, and the payment terms and conditions.

All payments must be made in full to CCC. For payment instructions, please see information listed at the bottom of this form.

License Number 2385980058885
License Date Mar 11, 2010

Licensed content publisher American Chemical Society
Licensed content publication Chemical Reviews
Licensed content title State of Understanding of Nafion
Licensed content author Kenneth A. Mauritz et al.
Licensed content date Oct 1, 2004
Volume number 104
Issue number 10
Type of Use Thesis/Dissertation
Requestor type Not specified
Format Print and Electronic
Portion Table/Figure/Chart
Number of Table/Figure /Charts
1
Author of this ACS article No
Order reference number
Title of the thesis / dissertation
Synthesis and Characterization of Purely Sulphonated Polysiloxane and Composite Membranes for High Temperature Fuel Cells
Expected completion date Apr 2010
Estimated size(pages) 80
Billing Type Invoice
Billing Address 103074 10th Sideroad
RR#4
Grand Valley, ON L0N 1G0
Canada
Customer reference info
Total 0.00 USD